Teleportation-Based Quantum Computation, Extended Temperley–Lieb Diagrammatical Approach and Yang–Baxter Equation

Yong Zhang [a,1], Kun Zhang [a,2], and Jinglong Pang [b,3]

[a] School of Physics and Technology, Wuhan University, P.R. China 430072
[b] Department of Physics, Peking University, P.R. China 100871

Abstract

This paper focuses on the study of topological features in teleportation-based quantum computation as well as aims at presenting a detailed review on teleportaiton-based quantum computation (Gottesman and Chuang, Nature 402, 390, 1999). In the extended Temperley–Lieb diagrammatical approach, we clearly show that such topological features bring about the fault-tolerant construction of both universal quantum gates and four-partite entangled states more intuitive and simpler. Furthermore, we describe the Yang–Baxter gate by its extended Temperley–Lieb configuration, and then study teleportation-based quantum circuit models using the Yang–Baxter gate. Moreover, we discuss the relationship between the extended Temperley–Lieb diagrammatical approach and the Yang–Baxter gate approach. With these research results, we propose a worthwhile subject, the extended Temperley–Lieb diagrammatical approach, for physicists in quantum information and quantum computation.

Key Words: Teleportation, Quantum Computation, Temperley–Lieb algebra, Yang–Baxter Equation

PACS numbers: 03.67.Lx, 03.65.Ud, 02.10.Kn

[1] yong_zhang@whu.edu.cn
[2] kun_zhang@whu.edu.cn
[3] jlpang@pku.edu.cn

1 Introduction

Quantum information and computation [1, 2] is an interdisciplinary research field of applying fundamental principles of quantum mechanics to information science and computer science. It represents a further development of quantum mechanics, and indeed helps us to achieve deeper understandings on quantum physics. Quantum entanglement [3, 4] as a fundamental concept of distinguishing classical physics from quantum physics has become a widely exploited resource in quantum information and computation. It has been experimentally verified that, under the assistance of quantum entanglement, an unknown qubit can be transmitted from Alice to Bob without any non-local physical interaction between them, using the quantum information protocol called quantum teleportation [5, 6, 7, 8]. Hence both quantum entanglement and quantum teleportation oblige quantum physicists to think about the relationship between Einstein's locality and quantum non-locality [3, 4].

Fault-tolerant quantum computation [1, 2] is required in practice to overcome decoherence, and teleportation-based quantum computation [9, 10, 11, 12, 13] is a powerful approach to fault-tolerant quantum computation in which universal quantum gate set is protected from noise using the teleportation protocol. Besides this, teleportation-based quantum computation is an example of measurement-based quantum computation which exploits quantum measurement as the main computing resource to determine which quantum gate is to be performed. In quantum mechanics, quantum measurement breaks quantum coherence and is usually performed at the end of an experiment, so measurement-based quantum computation essentially changes our conventional viewpoint on quantum measurement and also on the standard quantum circuit model [10] in which a coherent unitary dynamics is mainly involved.

As the title of this paper claims, we apply the extended Temperley–Lieb diagrammatical approach and the Yang–Baxter gate approach to the reformulation of teleportation-based quantum computation. The Temperley–Lieb algebra [14] is a well known concept in both statistical mechanics and low dimensional topology [15], and the Yang–Baxter equation [16] arises in exactly solving both some $1+1$-dimensional quantum many-body systems and vertex models in statistics physics. The fact [15] that a type of solutions of the Yang–Baxter equation can be constructed using the Temperley–Lieb algebra motivates the authors to explore teleportation-based quantum computation using the two related approaches.

The extended Temperley–Lieb diagrammatical approach [17, 18] is an extension of the standard diagrammatical representation of the Temperley–Lieb algebra, and with it, a quantum information protocol involving bipartite maximally entangled states, such as quantum teleportation, has a very nice topological diagrammatical interpretation. The Yang–Baxter gates are nontrivial unitary solutions of the Yang–Baxter equation, and the Yang–Baxter gate approach [19, 20, 21] to quantum information and computation is an algebraic method originally motivated by the observation that topological entanglements (like braiding configurations [15]) and quantum entanglements may have a kind of connection. Therefore, our research is expected to be interesting for physicists in quantum information and computation, which shows that teleportation-based quantum computation admits both topological and algebraic descriptions besides its standard description in quantum circuit model [9, 10, 11].

As we have introduced, we are going to go directly into at least three different research subjects in this paper, including quantum information and computation, the Temperley–Lieb algebra and the Yang–Baxter equation. The guiding principle of this kind of interdisciplinary research is that we want to explore the nature of quantum entanglement (quantum non-locality [3, 4]). As a matter of fact, nowadays, nobody is able to state that the nature of quantum entanglement has been fully understood [1, 2]. In accordance with [22], we study the nature of quantum entanglement by setting up a link between quantum entanglement (quantum non-locality) and topological entanglement (topological non-locality [15]).

Topological entanglement in the paper is represented by the extended Temperley–Lieb diagrammatical configuration or the Yang–Baxter gate configuration (the braiding configuration),

while quantum entanglement is represented by bipartite maximally entangled two-qubit pure states, i.e., the Bell states [1, 2]. In the extended Temperley–Lieb diagrammatical approach [17, 18], both the Bell states and Bell measurements have the Temperley–Lieb diagrammatical configurations on which quantum gates are allowed to move from this qubit to that qubit. In the Yang–Baxter gate approach [19, 20, 21], the algebraic formulation of teleportation-based quantum computation admits the braiding configuration on which quantum gates are permitted to move. Especially, the relationship between such the two approaches will be clarified in this paper.

The complete scheme of teleportation-based quantum computation was proposed by Gottesman and Chuang [9] in a very brief style, so it is necessary firstly to make a detailed review on teleportation-based quantum computation, topics including quantum teleportation, the fault-tolerant construction of universal quantum gate set and the fault-tolerant preparation of four-qubit entangled states. Then we present a topological diagrammatical description of such the reviewed topics in the extended Temperley–Lieb diagrammatical approach. Afterwards, we concentrate on the Yang–Baxter gates which are the Bell transform, a unitary basis transformation from the product basis to the Bell states, and with the help of our previous research on teleportation-based quantum computation using the Bell transform [13], we go into the algebraic description of teleportation-based quantum computation in terms of the Yang–Baxter gate. Finally, in view of the extended Temperley–Lieb diagrammatical representation of the Yang–Baxter gate, we set up a transparent link between the extended Temperley–Lieb diagrammatical approach and the Yang–Baxter gate approach.

Our study in this paper is meaningful and useful in the following sense. First, as we have emphasized, we try to dig out the nature of quantum non-locality from the viewpoint of topological non-locality. Second, the topological features in teleportation-based quantum computation make the fault-tolerant construction of both universal quantum gate set and four-qubit entangled states more intuitive and simpler. Third, we develop the concept of teleportation operator [13] in the Yang–Baxter gate approach to catch the intrinsic characteristic of quantum teleportation, which is capable of including the algebraic formulations of all possible teleportaiton processes. Fourth, the methodologies underlying our research are expected to be applied to other subjects in quantum information and computation, see Section 7 for concluding remarks on further research. Fifth, our research is expected to shed a light on further research in mathematical physics, see Appendix A.

It is obvious that what we have done in this paper is an interdisciplinary research among quantum information and computation, the low-dimensional topology and mathematical physics such as the Yang–Baxter equation. But we aim at introducing both the Temperley–Lieb algebra and the Yang–Baxter equation to physicists in quantum information and computation, in other words, readers can go through the entire paper without the preliminary knowledge on concepts in mathematical physics. All the results about both the Temperley–Lieb algebra and the Yang–Baxter equation are collected in Appendix A. Furthermore, for experts in mathematical physics, Appendix A.6 indeed presents a list of open problems for further research which are based on our reformulation of teleportation-based quantum computation.

This paper is organized as follows. Section 2 is a review on teleportation-based quantum computation [9]. Section 3 focuses on the topological diagrammatical description of teleportation-based quantum computation in the extended Temperley–Lieb diagrammatical approach. Section 4 presents the extended Temperley–Lieb configurations of two types of Yang–Baxter gates derived in Appendix A. Section 5 describes the Yang–Baxter gate approach to teleportation-based quantum computation. Section 6 clarifies the relationship between the extended Temperley–Lieb diagrammatical approach and the Yang–Baxter gate approach. To make the paper self-consistent, we present five appendices for readers' conveniences. Appendix A reviews both the Temperley–Lieb algebra and the Yang–Baxter equation as well as presents a detailed construction on the Yang–Baxter gate via the Temperley–Lieb algebra. Appendix B collects interesting properties of the permutation-like Yang–Baxter gates. Both Appendix C and Appendix D present the topological diagrammatical construction of four-qubit entangled states respectively associated with

the $CNOT$ gate and CZ gate [1]. Appendix E is about a method of calculating the extended Temperley–Lieb diagrammatical representation of the teleportation operator.

2 Review on teleportation-based quantum computation

In this section, we make a review on teleportation-based quantum computation [9]. The key topics include the standard description of quantum teleportation, the fault-tolerant construction of universal quantum gate set, and the fault-tolerant construction of four-qubit entangled states. Meanwhile, we set up our notation and convention for the study in the paper.

2.1 Notation

A single-qubit Hilbert space $\mathcal{H}_2$ has an orthonormal basis denoted by $|i\rangle$, $i = 0, 1$, and a single-qubit state $|\alpha\rangle$ is given by $|\alpha\rangle = a|0\rangle + b|1\rangle$ with complex numbers a and b. The unit matrix $\mathbb{1}_2$ and the Pauli gates X and Z take the form

$$\mathbb{1}_2 = \begin{pmatrix} 1 & 0 \\ 0 & 1 \end{pmatrix}, \quad X = \begin{pmatrix} 0 & 1 \\ 1 & 0 \end{pmatrix}, \quad Z = \begin{pmatrix} 1 & 0 \\ 0 & -1 \end{pmatrix} \tag{1}$$

with $Z|0\rangle = |0\rangle$ and $Z|1\rangle = -|1\rangle$, and the Pauli gate Y is defined as $Y = ZX$. A single-qubit gate is an element of the unitary group $U(2)$, and a typical single-qubit gate W_{ij} in the present paper has the form

$$W_{ij} = X^i Z^j, \quad i, j = 0, 1, \tag{2}$$

satisfying $W_{ij}^T = W_{ij}^\dagger$, in which the upper index T denotes the matrix transpose conjugation and the upper index † denotes the matrix Hermitian conjugation.

A two-qubit Hilbert space $\mathcal{H}_2 \otimes \mathcal{H}_2$ has an orthonormal product basis denoted by $|ij\rangle, i, j = 0, 1$. The EPR state $|\Psi\rangle$ [3, 4] takes the form

$$|\Psi\rangle = \frac{1}{\sqrt{2}}(|00\rangle + |11\rangle) \tag{3}$$

and it has a very nice algebraic property

$$(\mathbb{1}_2 \otimes U)|\Psi\rangle = (U^T \otimes \mathbb{1}_2)|\Psi\rangle \tag{4}$$

with U denoting any single-qubit gate. The set of the orthonormal Bell states $|\psi(ij)\rangle$ given by

$$|\psi(ij)\rangle = (\mathbb{1}_2 \otimes W_{ij})|\Psi\rangle, \quad i, j = 0, 1 \tag{5}$$

is called the Bell basis [1, 2] of the two-qubit Hilbert space $\mathcal{H}_2 \otimes \mathcal{H}_2$. Obviously, $|\Psi\rangle = |\psi(00)\rangle$.

2.2 Quantum teleportation

Let Alice and Bob share the EPR state $|\Psi\rangle$, and Alice wants to transfer an unknown quantum state $|\alpha\rangle$ to Bob. Alice and Bob prepare the quantum state $|\alpha\rangle \otimes |\Psi\rangle$ which can be formulated as

$$|\alpha\rangle \otimes |\Psi\rangle = \frac{1}{2} \sum_{i,j=0}^{1} |\psi(ij)\rangle \otimes W_{ij}|\alpha\rangle \tag{6}$$

which was called the teleportation equation in [18]. Then, Alice performs the Bell measurements $|\psi(ij)\rangle\langle\psi(ij)| \otimes \mathbb{1}_2$ on the prepared state $|\alpha\rangle \otimes |\Psi\rangle$,

$$(|\psi(ij)\rangle\langle\psi(ij)| \otimes \mathbb{1}_2)(|\alpha\rangle \otimes |\Psi\rangle) = \frac{1}{2}|\psi(ij)\rangle \otimes W_{ij}|\alpha\rangle, \tag{7}$$

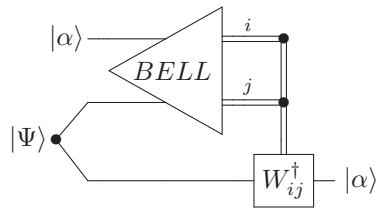

Figure 1: Quantum circuit for quantum teleportation as a diagrammatical representation of the teleportation equation (6). An unknown qubit $|\alpha\rangle$ is sent from Alice to Bob. The top two lines represent Alice's system and the bottom line represents Bob's system. The single-lines denote qubits and the double-lines denote classical bits. The triangle box represents the Bell measurement performed by Alice and the square box represents the local unitary correction operator $W_{ij}^{\dagger}$ performed by Bob to obtain the transmitted state $|\alpha\rangle$.

and she informs Bob her measurement results labeled as (i, j). Finally, Bob applies the unitary correction operator $W_{ij}^{\dagger}$ on his state

$$(\mathbb{1}_2 \otimes \mathbb{1}_2 \otimes W_{ij}^{\dagger})(|\psi(ij)\rangle \otimes W_{ij}|\alpha\rangle) = |\psi(ij)\rangle \otimes |\alpha\rangle \tag{8}$$

to obtain the transmitted quantum state $|\alpha\rangle$. See Figure 1 for the description of the teleportation protocol in the language of quantum circuit.

Note that the teleportation protocol of Bob transmitting an unknown qubit $|\alpha\rangle$ to Alice admits another type of the teleportation equation

$$|\Psi\rangle \otimes |\alpha\rangle = \frac{1}{2} \sum_{i,j=0}^{1} W_{ij}^{T}|\alpha\rangle \otimes |\psi(ij)\rangle \tag{9}$$

which was called the transpose teleportation equation in [13] and is to be used in the fault-tolerant construction of two-qubit gates in Subsubsection 2.3.4.

2.3 Fault-tolerant construction of universal quantum gate set

Quantum gates [23] are defined as unitary transformation matrices acting on quantum states, and the set of all n-qubit gates forms a representation of the unitary group $U(2^n)$.

2.3.1 Universal quantum gate set

An entangling two-qubit gate [24] with single-qubit gates is called a universal quantum gate set which can perform universal quantum computation in the circuit model [1] of quantum computation. All single-qubit gates can be generated by both the Hadamard gate H given by

$$H = \frac{1}{\sqrt{2}}(X + Z), \tag{10}$$

and the $\pi/8$ gate [25] given by

$$T = \begin{pmatrix} 1 & 0 \\ 0 & e^{i\frac{\pi}{4}} \end{pmatrix}. \tag{11}$$

An entangling two-qubit gate [24] is defined as a two-qubit gate capable of transforming a tensor product of two single-qubit states into an entangling two-qubit state. For examples, the $CNOT$ gate

$$CNOT = |0\rangle\langle 0| \otimes \mathbb{1}_2 + |1\rangle\langle 1| \otimes X, \tag{12}$$

and the CZ gate

$$CZ = |0\rangle\langle 0| \otimes \mathbb{1}_2 + |1\rangle\langle 1| \otimes Z. \tag{13}$$

They are maximally entangling gates [26], namely, with single-qubit gates, they can generate the maximally entangling states such as the Bell states (5) from the product states. The $CNOT$ gate is the well known two-qubit gate in quantum information and computation which is the quantum analogue of the Exclusive OR gate in classical computation [1]. The CZ gate is widely used in the one-way quantum computation [27], the representative example of measurement-based quantum computation, and it is related to the $CNOT$ gate in the way

$$CZ = (\mathbb{1}_2 \otimes H)CNOT(\mathbb{1}_2 \otimes H) \equiv H_2\ CNOT\ H_2 \tag{14}$$

in which the subscript of the Hadamard gate H means that it is acting on the second qubit. Hence the set of the $CNOT$ gate (12) (or the CZ gate (13)) with single-qubit gates H (10) and T (11) is called a universal quantum gate set to perform universal quantum computation [1].

2.3.2 Clifford gates and fault-tolerant quantum computation

The Pauli group gates C_1 are generated by tensor products of the Pauli matrices X, Z and the identity matrix $\mathbb{1}_2$ with global phase factors $\pm 1, \pm i$. Quantum gates U [1] are classified by

$$C_k \equiv \{U | UC_{k-2}U^\dagger \subseteq C_{k-1}\} \tag{15}$$

where C_2 denotes the Clifford gates preserving the Pauli group gates under conjugation. Obviously, the Hadamard gate H is a Clifford gate, namely $H \in C_2$, due to

$$HXH = Z, \quad HZH = X, \tag{16}$$

and the $\pi/8$ gate T is not a Clifford gate, $T \in C_3$, since

$$TXT^\dagger = \frac{X - \sqrt{-1}Y}{\sqrt{2}}, \quad TZT^\dagger = Z \tag{17}$$

in which $(X - \sqrt{-1}Y)/\sqrt{2}$ is a Clifford gate [1, 28]. Here is another equivalent definition of the Clifford gate [1, 28]. If a quantum gate can be represented as a tensor product of the Hadamard gate (10), the phase gate

$$S = \begin{pmatrix} 1 & 0 \\ 0 & i \end{pmatrix}, \tag{18}$$

and the $CNOT$ gate (12), then it is a Clifford gate. Note that the phase gate S is the square of the $\pi/8$ gate (11), $S = T^2$, and the square of the phase gate S is the Pauli Z gate, $S^2 = Z$.

In fault-tolerant quantum computation [28], the Pauli group gates C_1 and Clifford gates C_2 can be easily performed in principle, but the C_3 gates may be difficultly realized. The teleportation-based quantum computation [9] is fault-tolerant quantum computation in the following sense: to perform a C_3 gate, it prepares a quantum state with the action of C_3 gate and then applies C_1 or C_2 gates to such the quantum state using the teleportation protocol.

2.3.3 Fault-tolerant construction of single-qubit gates

To perform a single-qubit gate $U \in C_k$ (15) on the unknown state $|\alpha\rangle$, Alice prepares the quantum state $|\Psi_U\rangle$ given by

$$|\Psi_U\rangle = (\mathbb{1}_2 \otimes U)|\Psi\rangle \tag{19}$$

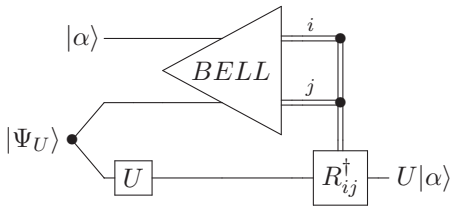

Figure 2: Quantum circuit for the fault-tolerant construction of the single-qubit gate U associated with the teleportation equation (20). With the such diagrammatical representation, it is obvious that fault-tolerantly implementing the single-qubit U becomes how to fault-tolerantly perform the $R_{ij}^{\dagger}$ gate and prepare the preliminary quantum state $|\Psi_U\rangle$ (19).

and reformulate $|\alpha\rangle \otimes |\Psi_U\rangle$ as

$$|\alpha\rangle \otimes |\Psi_U\rangle = \frac{1}{2} \sum_{i,j=0}^{1} |\psi(ij)\rangle \otimes R_{ij} U |\alpha\rangle, \tag{20}$$

where the single-qubit gate R_{ij} has the form $R_{ij} = UW_{ij}U^{\dagger}$ with W_{ij} defined in (2). Then Alice makes Bell measurements $|\psi(ij)\rangle\langle\psi(ij)| \otimes \mathbb{1}_2$ and informs Bob her measurement results labeled by (i, j). Finally, Bob performs the unitary correction operator $R_{ij}^{\dagger} \in C_{k-1}$ (15) to attain $U|\alpha\rangle$. See Figure 2 for the quantum circuit of fault-tolerantly performing the single-qubit gate U using the teleportation protocol.

As the single-qubit gate U is the Hadamard gate H (10), the single-qubit gate R_{ij} is given by $R_{ij}(H) = W_{ji}^T$, which is a tensor product of Pauli gates. And as the single-qubit gate U is the $\pi/8$ gate (11), the single-qubit gate R_{ij} is given by

$$R_{ij}(T) = (\frac{X - \sqrt{-1}Y}{\sqrt{2}})^i \, Z^j, \tag{21}$$

which can be easily fault-tolerantly performed, because it is a Clifford gate. Note that the difficulty of performing a single-qubit gate $U \in C_k$ becomes how to fault-tolerantly prepare the state $|\Psi_U\rangle$ and perform the single-qubit gate $R_{ij}^{\dagger} \in C_{k-1}$.

2.3.4 Fault-tolerant construction of two-qubit Clifford gates

To perform a two-qubit Clifford gate CU such as the $CNOT$ gate (12) and the CZ gate (13) on two unknown single-qubit states $|\alpha\rangle$ and $|\beta\rangle$, we prepare a four-qubit entangled state $|\Psi_{CU}\rangle$,

$$|\Psi_{CU}\rangle = (\mathbb{1}_2 \otimes CU \otimes \mathbb{1}_2)(|\Psi\rangle \otimes |\Psi\rangle), \tag{22}$$

with the action of the CU gate, and reformulate the prepared state $|\alpha\rangle \otimes |\Psi_{CU}\rangle \otimes |\beta\rangle$ as

$$\begin{aligned} &|\alpha\rangle \otimes |\Psi_{CU}\rangle \otimes |\beta\rangle \\ =&\frac{1}{4} \sum_{i_1,j_1=0}^{1} \sum_{i_2,j_2=0}^{1} (\mathbb{1}_4 \otimes Q \otimes P \otimes \mathbb{1}_4)(|\psi(i_1 j_1)\rangle \otimes CU|\alpha\beta\rangle \otimes |\psi(i_2 j_2)\rangle) \end{aligned} \tag{23}$$

with $\mathbb{1}_4 = \mathbb{1}_2 \otimes \mathbb{1}_2$, which is called the teleportation equation associated with the fault-tolerant construction of the two-qubit Clifford gate CU.

The single-qubit gates Q and P in the teleportation equation (23) are calculated by

$$Q \otimes P = CU(W_{i_1 j_1} \otimes W_{i_2 j_2}^T)CU^{\dagger}. \tag{24}$$

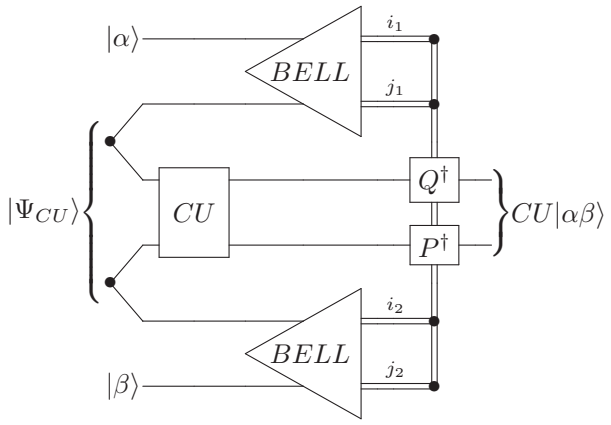

Figure 3: Quantum circuit for the fault-tolerant construction of a two-qubit Clifford gate CU, as a diagrammatical representation of the teleportation equation (23). Specifically, the single-qubit gates Q and P are calculated with the formula (24).

As the CU gate is the $CNOT$ gate, the gates Q and P are expressed as

$$Q = Z^{j_2} X^{i_1} Z^{j_1}, \quad P = Z^{j_2} X^{i_2} X^{i_1}. \tag{25}$$

As the CU gate is the CZ gate, the gates Q and P have the form

$$Q = Z^{i_2} X^{i_1} Z^{j_1}, \quad P = Z^{j_2} X^{i_2} Z^{i_1}. \tag{26}$$

Note that the Q and P gates (24) may be not single-qubit gates if the CU gate is not a Clifford gate in accordance with the definition of a Clifford gate [1, 28].

Next, we perform the Bell measurements given by

$$|\psi(i_1 j_1)\rangle\langle\psi(i_1 j_1)| \otimes \mathbb{1}_2 \otimes \mathbb{1}_2 \otimes |\psi(i_2 j_2)\rangle\langle\psi(i_2 j_2)|, \tag{27}$$

and with the measurement results labeled by (i_1, j_1) and (i_2, j_2), we perform the unitary correction operator, $Q^\dagger \otimes P^\dagger$, to obtain the exact action of the Clifford gate CU on the two-qubit state $|\alpha\rangle \otimes |\beta\rangle$, namely, $CU|\alpha\beta\rangle$.

The quantum circuit for the fault-tolerant construction of the two-qubit Clifford gate CU using the teleportation protocol is depicted in Figure 3. Note that the two-qubit Clifford gate CU we study here may be not the controlled-operation two-qubit gates such as the $CNOT$ gate (12) and the CZ gate (13).

2.4 Construction of four-qubit entangled states

From Subsection 2.3, we already know that, the conceptual point in the fault-tolerant construction of a single-qubit quantum gate U (or a two-qubit Clifford gate CU) using quantum teleportation is the fault-tolerant preparation of the two-qubit entangled state (19) (or the four-qubit entangled state (22)). In this subsection, we focus on the fault-tolerant preparation of the four-qubit entangled state $|\Psi_{CU}\rangle$ (22) using the teleportation protocol, when the CU gate is the $CNOT$ gate (12) and the CZ gate (13) respectively.

In Gottesman and Chuang's original proposal [9] of teleportation-based quantum computation, a four-qubit entangled state $|\Psi_{CU}\rangle$ is prepared in the following steps. First, we prepare a prior entangled six-qubit state as a tensor product of a three-qubit GHZ state $|\Upsilon\rangle$ [29],

$$|\Upsilon\rangle = \frac{1}{\sqrt{2}}(|000\rangle + |111\rangle) \tag{28}$$

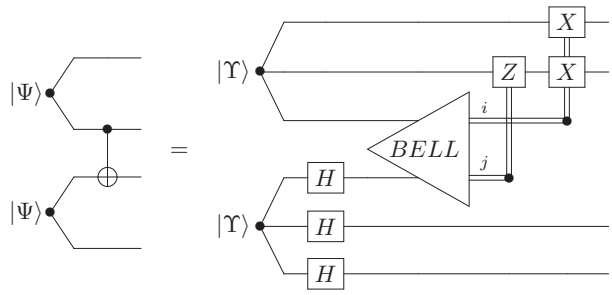

Figure 4: Quantum circuit for the construction of four-qubit entangled state $|\Psi_{CNOT}\rangle$ (29), as a diagrammatical representation of the teleportation equation (30). The $|\Upsilon\rangle$ state is the three-quibt GHZ state (28) and the single-qubit gate denoted as H is the Hadamard gate (10). The $CNOT$ gate (12) takes the conventional configuration in quantum circuit model [1].

and another three-qubit GHZ state $|\Upsilon\rangle$ with the local action of the Hadamard gate H. Second, we perform the Bell measurements on such the six-qubit entangled state. Third, after classical communication of the Bell measurement outcomes, we perform the unitary correction operators to obtain the four-qubit entangled state $|\Psi_{CU}\rangle$.

2.4.1 Construction of the four-qubit entangled state $|\Psi_{CNOT}\rangle$

The four-qubit entangled state $|\Psi_{CNOT}\rangle_{1256}$ is the target state we want to construct,

$$|\Psi_{CNOT}\rangle_{1256} = (\mathbb{1}_2 \otimes CNOT_{25} \otimes \mathbb{1}_2)(|\Psi\rangle_{12} \otimes |\Psi\rangle_{56}) \tag{29}$$

in which the $CNOT_{ij}$ gate requires the i-th qubit as the control qubit and the j-th qubit as the target qubit. We prepare the six-qubit entangled state $H_4H_5H_6|\Upsilon\rangle_{123}|\Upsilon\rangle_{456}$, which can be reformulated as

$$H_4H_5H_6|\Upsilon\rangle_{123}|\Upsilon\rangle_{456} = \sum_{i,j=0}^{1} |\psi(ij)\rangle_{34}\ Z_2^j X_1^i X_2^i |\Psi_{CNOT}\rangle_{1256}, \tag{30}$$

then make the joint Bell measurement on both the third and fourth qubits given by

$$\mathbb{1}_2 \otimes \mathbb{1}_2 \otimes |\psi(ij)\rangle_{34}\langle\psi(ij)| \otimes \mathbb{1}_2 \otimes \mathbb{1}_2. \tag{31}$$

With the measurement outcome (i, j), we perform the unitary correction operator

$$X^i \otimes X^i Z^j \otimes \mathbb{1}_2 \otimes \mathbb{1}_2 \otimes \mathbb{1}_2 \otimes \mathbb{1}_2, \tag{32}$$

on the resultant quantum state to obtain the four-qubit entangled state $|\Psi_{CNOT}\rangle$ (29). The quantum circuit for the construction of the $|\Psi_{CNOT}\rangle$ state is shown in Figure 4.

Note that the teleportation equation (30) admits an equivalent form

$$H_4H_5H_6|\Upsilon\rangle_{123}|\ \Upsilon\rangle_{456} = \sum_{i,j=0}^{1} |\psi(ij)\rangle_{34}\ X_5^i Z_5^j Z_6^j |\Psi_{CNOT}\rangle_{1256}, \tag{33}$$

so that we have the second method of constructing the $|\Psi_{CNOT}\rangle$ state (29) using the teleportation protocol. These two methods are found to be equivalent in the low dimensional topological diagrammatical approach, see Subsubsection 3.4.2.

2.4.2 Construction of four-qubit entangled states $|\Psi^{\uparrow}_{CNOT}\rangle$ and $|\Psi_{CZ}\rangle$

In Gottesman and Chuang's original study [9], the fault-tolerant construction of the four-qubit entangled state $|\Psi^{\uparrow}_{CNOT}\rangle$ (180) was presented instead of the state $|\Psi_{CNOT}\rangle$ (29) that we are working on. For readers' convenience, the construction of the $|\Psi^{\uparrow}_{CNOT}\rangle$ state is discussed in Appendix C. Besides $|\Psi_{CNOT}\rangle$ and $|\Psi^{\uparrow}_{CNOT}\rangle$, since the CZ gate (13) has a wide application in measurement-based quantum computation [27], we work out the construction of four-qubit entangled state $|\Psi_{CZ}\rangle$ (188) in Appendix D.

3 The extended Temperley–Lieb diagrammatical approach to teleportation-based quantum computation

In this section[4], we aim at exhibiting topological features of teleportation-based quantum computation in the transparent style. In the extended Temperley–Lieb diagrammatical approach [17, 18], we study the topological diagrammatical construction of both universal quantum gate set and four-qubit entangled states in teleportation-based quantum computation [9, 10, 11], whose algebraic counterparts have been presented in Section 2.

The extended Temperley–Lieb diagrammatical configuration [17, 18] is a kind of the extension of the standard Temperley–Lieb configuration on which both single-qubit gates and two-qubit gates are allowed to move along the lines under certain rules. The definition of the Temperley–Lieb algebra and its diagrammatical representation is shown up in Appendix A.1 and A.2.

3.1 The extended Temperley–Lieb diagrammatical approach

A single-qubit state vector $|\varphi\rangle$ is denoted by a vertical line followed by the symbol ∇ on the bottom,

$$|\varphi\rangle = \quad \downarrow \nabla \tag{34}$$

and the line with the symbol $\triangle$ on the top represents the covector $\langle\phi|$, so a vertical line with both symbols ∇ and $\triangle$ on the boundary denotes the inner product $\langle\phi|\varphi\rangle$. A vertical line with a solid point represents a single-qubit gate U acting on the state $|\varphi\rangle$,

$$U|\varphi\rangle = \quad \downarrow U \nabla \tag{35}$$

in which the algebraic expression is read from the right to the left and the diagrammatical representation is read from the bottom to the top.

The diagrammatical configuration of the Bell state $|\psi(ij)\rangle$ (5) is the core of the extended Temperley–Lieb diagrammatical approach, and it is represented by a cup with a solid point denoting the single-qubit gate W_{ij} (2),

$$|\psi(ij)\rangle = \quad \sqcup_{W_{ij}} \tag{36}$$

so that a cup without a solid point denotes the EPR state $|\Psi\rangle$ (3). The adjoint of the Bell state, $\langle\psi(ij)|$, is represented by a cap

$$\langle\psi(ij)| = \quad \sqcap_{W^{\dagger}_{ij}} \tag{37}$$

[4]This section is an extended version of the authors' unpublished paper [12] in which topological features of teleportation-based quantum computation are claimed to be associated with topological features of space-time.

with a solid point denoting the Hermitian conjugation of W_{ij}. These diagrammatic states are called a cup state or a cap state respectively. The projective measurement $|\psi(ij)\rangle\langle\psi(ij)|$ is called the Bell measurement,

$$|\psi(ij)\rangle\langle\psi(ij)| = \tag{38}$$

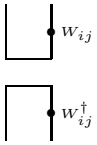

represented by a top cup state with a bottom cap state. Note that without solid points on the configuration of the Bell measurement, such the configuration represents the basic generator of the Temperley–Lieb algebra, see Appendix A.1 and A.2.

The nice property (4) of the EPR state has the corresponding diagrammatical expression

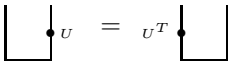

(39)

with U denoting any single-qubit gate, and the similar representation also for a cap state,

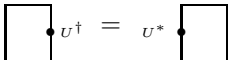

(40)

with the upper index $*$ denoting the complex conjugation. In the diagrammatical representations (39) and (40), a single-qubit gate can flow from the one branch of a cup (or cap) state to its other branch with the transpose conjugation, which is beyond the conventional utilization of the Temperley–Lieb diagrams but naturally arises in quantum computation. Note that such the operation of moving single-qubit gates is a crucial technique in the extended Temperley–Lieb diagrammatical approach [17, 18] to teleportation-based quantum circuits.

3.2 Topological interpretation of quantum teleportation

In quantum teleportation, Alice and Bob prepare the quantum state $|\alpha\rangle \otimes |\Psi\rangle$, in the extended Temperley–Lieb diagrammatical language, expressed as

$$|\alpha\rangle \otimes |\Psi\rangle = \tag{41}$$

in which the vertical line with ∇ denotes the unknown quantum state $|\alpha\rangle$ to be transmitted from Alice to Bob. Then, Alice performs Bell measurements $|\psi(ij)\rangle\langle\psi(ij)| \otimes \mathbb{1}_2$ on the prepared state $|\alpha\rangle \otimes |\Psi\rangle$, which has the extended Temperley–Lieb diagrammatical configuration

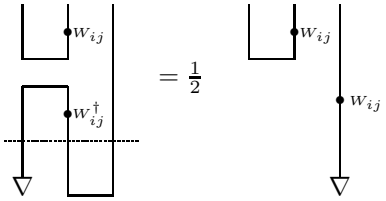

(42)

with the single-qubit gate W_{ij} defined in (2). It is obvious that this topological diagram (42) is associated with both the teleportation equation (6) and the quantum circuit in Figure 1. Note that the diagram (42) without solid points is a standard diagrammatical representation of the Temperley–Lieb algebra [15], see Appendix A.1 and A.2.

Now let us explain the diagram (42) in detail. On the left hand side of $=$, the diagrammatical part above the dashed line denotes the Bell measurement, and the part under the dashed line denotes the state preparation. On the right hand side of $=$, the normalization factor $\frac{1}{2}$ is contributed by the vanishing cup state and cap state according to the rules of the extend Temperley–Lieb diagrammatical approach [17, 18]. The cup state with the action of W_{ij} denotes the post-measurement state which is usually neglected in the following study for simplicity. The W_{ij} gate acting on the unknown qubit $|\alpha\rangle$ is due to the operation of moving $W_{ij}^{\dagger}$ from the one branch of the cap state to the other branch and applying the transposition conjugation, $(W_{ij}^{\dagger})^{T} = W_{ij}$. Note that both classical communication and unitary correction are not shown in the diagram (42). In this sense, hence, the quantum information flow sending an unknown qubit from Alice to Bob in quantum teleportation can be recognized as a result of topological operation in the extended Temperley–Lieb diagrammatical approach [17, 18].

The topology in the diagrammatical teleportation (42) may be not that obvious. Let us consider the topological configuration of the chained teleportation [30] that Alice sends an unknown qubit $|\alpha\rangle$ to Bob with a sequence of standard teleportation protocols, expressed as

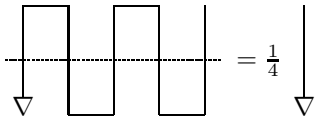

(43)

in which the post-measurement states are neglected and only the EPR state measurements $|\Psi\rangle\langle\Psi|$ are considered. The normalization factor $\frac{1}{4}$ is calculated from two vanishing cup states and two vanishing cap states. Without unitary corrections, Bob obtains the exact quantum state $|\alpha\rangle$. Hence *the teleportation topology in the extended Temperley–Lieb diagrammatical approach is defined as a topological operation which straightens the configuration consisting of cap states and cup states*. In addition, if we perform the Bell measurements $|\psi(ij)\rangle\langle\psi(ij)|$ instead of the EPR state measurements in the chained teleportation, first of all, we have to move single-qubit gates along the path formed by top cap states with bottom cup states until boundary points of this path under the guidance of the properties (39) and (40), and then apply the topological operation by straightening the relevant configuration.

3.3 Topological construction of universal quantum gate set

In the authors' knowledge, a topological diagrammatical construction of universal quantum gate set [1, 23] using quantum teleportation [9] has not been done yet in the published paper, so we study such the realization in the extended Temperley-Lieb diagrammatical approach [17, 18].

The topological diagram for the fault-tolerant construction of a single-qubit U using quantum teleportation has the form

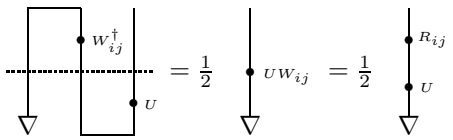

(44)

and it is directly associated with the teleportation equation (20) and the quantum circuit model in Figure 2, see Subsubsection 2.3.3. Below the dashed line, Alice and Bob prepare the quantum state $|\alpha\rangle\otimes|\Psi_U\rangle$, and above the dashed line, Alice performs the Bell measurements $|\psi(ij)\rangle\langle\psi(ij)|\otimes \mathbb{1}_2$. After moving the single-qubit gate $W_{ij}^{\dagger}$ from Alice to Bob, we straighten the configuration of the top cap with the bottom cup and obtain the normalization factor $\frac{1}{2}$. Obviously, Bob has to perform the local unitary correction operator $R_{ij}^{\dagger}$ to obtain the action of the single-qubit gate U on the unknown state $|\alpha\rangle$, namely, $U|\alpha\rangle$, as is not shown up in the topological diagram (44).

The topological diagram for the fault-tolerant construction of a two-qubit Clifford gate CU using quantum teleportation is expressed as

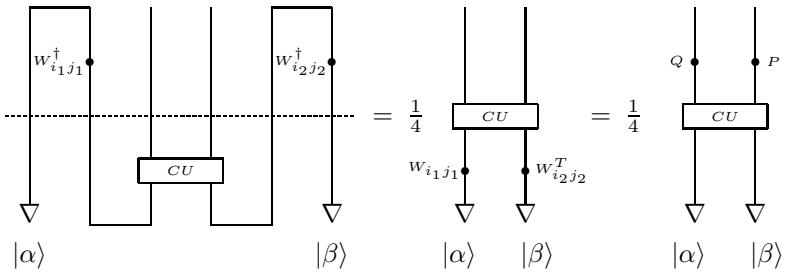

(45)

and it is associated with the teleportation equation (23) and the quantum circuit model in Figure 3. Below the dashed line, we prepare the six-qubit quantum state $|\alpha\rangle \otimes |\Psi_{CU}\rangle \otimes |\beta\rangle$, and above the dashed line, we perform the Bell measurement (27) on such the prepared quantum state. The topological (or straightening) operation occurs after both moving single-qubit gates $W^{\dagger}_{i_1 j_1}$ and $W^{\dagger}_{i_2 j_2}$ along the path formed by the top cup states and bottom cup states and moving the two-qubit gate CU along two vertical lines. The vanishing cap and cup states contribute the normalization factor $\frac{1}{4}$. Explicitly, the single-qubit gates Q and P are calculated by the formula (24).

As a remark, the extended Temperley–Lieb diagrammatical approach to the fault-tolerant construction of quantum gates in teleportation-based quantum computation appears more intuitive and simpler than other original approaches [9, 10, 11]. On the topological representations, such as (42), (44) and (45), one is allowed to transport an unknown quantum state by topological operations as well as move single-qubit or two-qubit gates along relevant configurations.

3.4 Topological construction of four-qubit entangled states

We combine the quantum circuit models [1] of the Bell states and the GHZ states with the extended Temperley–Lieb diagrammatical approach to construct the topological diagrammatical representations of four-qubit entangled states including the $|\Psi_{CNOT}\rangle$ state (29), the $|\Psi^{\uparrow}_{CNOT}\rangle$ state (180) and the $|\Psi_{CZ}\rangle$ state (188).

3.4.1 Diagrammatical representations of the Bell state $|\Psi\rangle$ and GHZ state $|\Upsilon\rangle$

The EPR state $|\Psi\rangle$ (3) can be generated by the quantum circuit model in terms of the Hadamard gate H and the $CNOT$ gate,

$$|\Psi\rangle = CNOT_{12}(H \otimes \mathbb{1}_2)|0\rangle \otimes |0\rangle \tag{46}$$

with the diagrammatic representation

$$|\Psi\rangle = \tag{47}$$

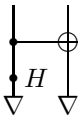

where the vertical line with ∇ denotes the state $|0\rangle$. Such the configuration of the EPR state $|\Psi\rangle$ is equivalent to the cup configuration (36) of the $|\Psi\rangle$ state in the extended Temperley–Lieb diagrammatical approach. The EPR state $|\Psi\rangle$ has the other equivalent quantum circuit model

$$|\Psi\rangle = CNOT_{21}(\mathbb{1}_2 \otimes H)|00\rangle \tag{48}$$

with the diagrammatical representation

$$|\Psi\rangle = \tag{49}$$

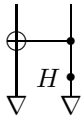

which is associated with the configuration (47) via the mirror symmetry.

The three-qubit GHZ state $|\Upsilon\rangle$ (28) can be generated by the quantum circuit model in terms of the EPR state $|\Psi\rangle$ and the $CNOT$ gate, expressed as

$$|\Upsilon\rangle = (CNOT_{21} \otimes \mathbb{1}_2)|0\rangle \otimes |\Psi\rangle, \tag{50}$$

with the diagrammatical representation

$$|\Upsilon\rangle = \tag{51}$$

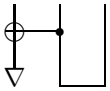

where the cup configuration (36) of the EPR state $|\Psi\rangle$ is exploited. The $|\Upsilon\rangle$ state also allows the other equivalent quantum circuit model

$$|\Upsilon\rangle = (\mathbb{1}_2 \otimes CNOT_{23})|\Psi\rangle \otimes |0\rangle, \tag{52}$$

with the diagrammatical representation

$$|\Upsilon\rangle = \tag{53}$$

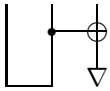

which can be obtained from the configuration (51) via the mirror symmetry.

Furthermore, the GHZ state $|\Upsilon\rangle$ with the local action of the Hadamard gates such as $(H \otimes H \otimes H)|\Upsilon\rangle$ has the diagrammatical representation,

$$= \tag{54}$$

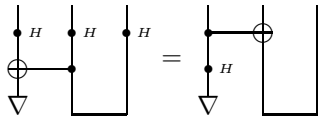

where the configuration (51) of the GHZ state $|\Upsilon\rangle$ is used and the formula

$$(H \otimes H)CNOT_{21}(H \otimes H) = CNOT_{12} \tag{55}$$

is applied. Under the mirror symmetry, the $(H \otimes H \otimes H)|\Upsilon\rangle$ state has the other equivalent configuration

$$= \tag{56}$$

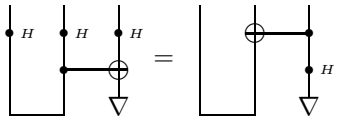

in which the configuration (53) of the GHZ state $|\Upsilon\rangle$ is exploited.

3.4.2 Topological construction of the four-qubit entangled state $|\Psi_{CNOT}\rangle$

The four-qubit entangled state $|\Psi_{CNOT}\rangle$ (29) has the extended Temperley–Lieb diagrammatical configuration, expressed as a $CNOT$ gate connecting two cup configurations,

$$|\Psi_{CNOT}\rangle = \tag{57}$$

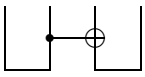

where the second qubit is the control qubit and the fifth qubit is the target qubit and both the third and fourth qubits are not explicitly shown up.

Following the strategy of constructing $|\Psi_{CNOT}\rangle$ (29) in Subsubsection 2.4.1, we perform the Bell measurements (31) on both the third and fourth qubits of the six-qubit state $|\Upsilon\rangle \otimes (H \otimes H \otimes H)|\Upsilon\rangle$. Using the diagrammatical representation (51) of the GHZ state $|\Upsilon\rangle$ and the diagrammatical representation (54) of the state $(H \otimes H \otimes H)|\Upsilon\rangle$ and the diagrammatical representation (38) of the Bell measurements (31), we have the extended Temperley–Lieb diagrammatical configuration for the construction of the $|\Psi_{CNOT}\rangle$ state (29),

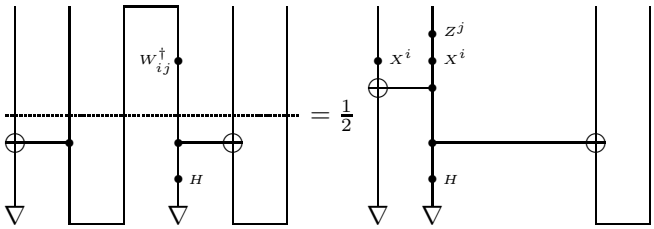

(58)

which is associated with the teleportation equation (30) and the quantum circuit model in Figure 4, and in which below the dashed line is the prepared six-qubit state and above the dashed line is the Bell measurements.

Let us perform a series of diagrammatical operations on the diagram (58). First, move the single-qubit gate $W_{ij}^{\dagger}$ from the fourth qubit to the second qubit along the given path. Second, continue to move such the $W_{ij}^{\dagger}$ gate across the $CNOT_{21}$ gate with the formula

$$CNOT_{21}(\mathbb{1}_2 \otimes W_{ij}^{\dagger})CNOT_{21} = Z_2^j X_1^i X_2^i, \tag{59}$$

to obtain the single-qubit gates $Z_2^j X_1^i X_2^i$ acting on the first and second qubits. Third, straighten the configuration of the bottom cup with the top cap between the second qubit and the fourth qubit to derive the normalization factor $\frac{1}{2}$ and meanwhile to obtain the $CNOT_{25}$ gate and the Hadamard gate H_2 respectively from the original $CNOT_{45}$ gate and the Hadamard gate H_4

Obviously, the $CNOT_{21}$ gate commutes with the $CNOT_{25}$ gate, and applying such the fact on the diagram (58) brings about the topological diagrammatical representation

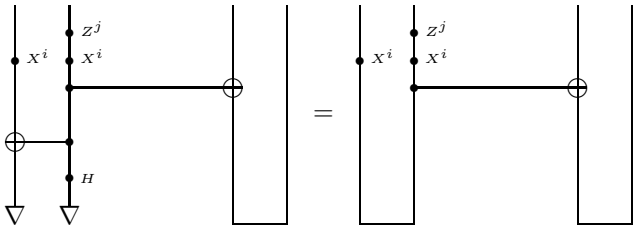

(60)

in which the diagrammatic representation (49) of the EPR state $|\Psi\rangle$ is used. With both classical communication and unitary correction, therefore, the extended Temperley–Lieb diagrammatical representation (57) of the four-qubit entangled state $|\Psi_{CNOT}\rangle$ can be exactly prepared in the diagrammatical approach.

Now let us derive the teleportation equation (33) in the topological diagrammatical approach. On the diagram (58), we replace the diagrammatical representation (51) of the GHZ state $|\Upsilon\rangle$ with its another diagrammatical representation (53) and replace the diagrammatical representation (54) of the $H_1H_2H_3|\Upsilon\rangle$ state with its another diagrammatical representation (56) so that we have the

other equivalent topological diagrammatical representation,

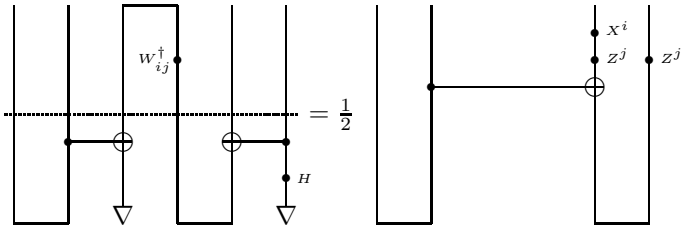

(61)

in which we firstly move the single-qubit gate $W_{ij}^{\dagger}$ from the fourth qubit to the fifth qubit and then across $CNOT_{65}$ gate with the formula

$$CNOT_{65}(W_{ij} \otimes \mathbb{1}_2)CNOT_{65} = X_5^i Z_5^j Z_6^j, \tag{62}$$

to generate the single-qubit gate $X_5^i Z_5^j Z_6^j$, and secondly apply the commutative relation of the $CNOT_{25}$ gate and $CNOT_{65}$ and the diagrammatic representation (49) of the EPR state $|\Psi\rangle$. As a result, the diagram (61) presents a kind of proof for the teleportation equation (33).

3.4.3 Topological constructions of four-qubit entangled states $|\Psi_{CNOT}^{\uparrow}\rangle$ and $|\Psi_{CZ}\rangle$

The topological constructions of the four-qubit entangled states $|\Psi_{CNOT}^{\uparrow}\rangle$ (180) and $|\Psi_{CZ}\rangle$ (188) are shown up in Appendix C and Appendix D respectively.

4 The Yang–Baxter gate and its extended Temperley–Lieb diagrammatical representation

In this section, we consider two special types of the Yang–Baxter gates derived in Appendix A as well as present their associated extended Temperley–Lieb diagrammatical configurations, and then apply the special type II Yang–Baxter gates to teleportation-based quantum computation in Section 5. Note that a brief study on the algebraic properties of the special type I Yang–Baxter gates is made in Appendix B. In the first place, the extended Temperley–Lieb diagrammatical representation of a two-qubit quantum gate will be discussed.

4.1 The extended Temperley-Lieb diagrammatical representation of a two-qubit gate

The conventional Temperley–Lieb diagram consists of the configuration of a pair of cup and cap [15], see Appendix A.1 for the diagrammatical representation of the Temperley–Lieb algebra. As we have introduced in Section 3, the extended Temperley–Lieb diagram permits the action of single-qubit gates, namely, it includes the following typical configuration,

$$|\Psi_M\rangle\langle\Psi_N| = \tag{63}$$

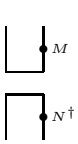

which represents the EPR state projector $|\Psi\rangle\langle\Psi|$ with the local action of single-qubit gates M and $N^{\dagger}$. Obviously, when $M = N = \mathbb{1}_2$, such the configuration (63) becomes the standard Temperley–Lieb configuration in Appendix A.1.

In quantum information and computation [1], the two-qubit Hilbert space $\mathcal{H}_2 \otimes \mathcal{H}_2$ has the two types of the orthonormal bases: the one is denoted by the product basis $|ij\rangle$, the other is

denoted by the Bell basis $|\psi(ij)\rangle$, and the unitary basis transformation matrix T between these two bases satisfies $T|ij\rangle = |\psi(ij)\rangle$ and has the form,

$$T = \frac{1}{\sqrt{2}} \begin{pmatrix} 1 & 1 & 0 & 0 \\ 0 & 0 & 1 & 1 \\ 0 & 0 & 1 & -1 \\ 1 & -1 & 0 & 0 \end{pmatrix}. \tag{64}$$

In terms of the product base $|ij\rangle\langle kl|$, a two-qubit quantum gate G as a 4×4 unitary matrix has an expression given by

$$G = \sum_{i,j,k,l=0}^{1} G_{ij,kl} |ij\rangle\langle kl|, \tag{65}$$

and in terms of the Bell base $|\psi(ij)\rangle\langle\psi(kl)|$, it has another form

$G = \sum_{i,j,k,l=0}^{1} \tilde{G}_{ij,kl}$ 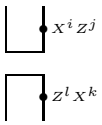

(66)

in the extended Temperley–Lieb diagrammatical approach. Applying the basis transformation matrix T (64), the coefficient matrix $\tilde{G} = (\tilde{G}_{ij,kl})$ can be obtained from

$$\tilde{G} = T^\dagger G T. \tag{67}$$

For example, the two-qubit identity gate $\mathbb{1}_4$ has an expansion of the Bell basis (5),

$$\mathbb{1}_4 = \sum_{i,j=0}^{1} |\psi(ij)\rangle\langle\psi(ij)|, \tag{68}$$

which represents the completeness relation defining the Bell basis, so the two-qubit identity gate $\mathbb{1}_4$ has the extended Temperley–Lieb diagrammatic representation,

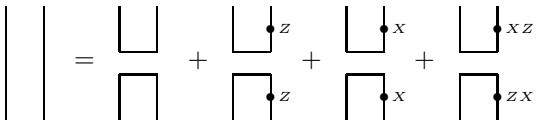

, (69)

where, in the conventional topological viewpoint [15], the two-qubit identity gate $\mathbb{1}_4$ is depicted as two parallel vertical lines.

For another example, let us consider the extended Temperley–Lieb diagrammatical configuration of the CZ gate (13), which is

$CZ =$ 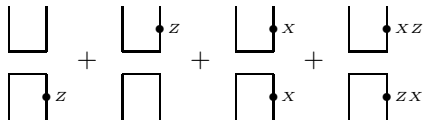

, (70)

where the first and second configurations from the left handside are explicitly beyond the standard Temperley–Lieb diagrammatical representation in Appendix A.1.

Note that for a given two-qubit gate G, its extended Tempereley–Lieb diagrammatical representation is not fixed and depends on the choices of single-qubit gates acting on the cup or cap configurations. For example, the extended Temperley–Lieb diagrammatic representation of the CZ gate (13) can not be (70) when single-qubit gates on the configurations are not the Pauli gates.

4.2 Special type I Yang–Baxter gate and its extended Temperley-Lieb diagrammatical representation

The special type I Yang–Baxter gate is a typical example for the Yang–Baxter gate via the Temperley–Lieb algebra, and it is derived in Appendix A.5.1. The main reason that we study it in this paper is that it is directly associated with the Bell states (5), and we denote the special type I Yang–Baxter gate by $R(ij)$, which is formulated as

$$R(ij) = \mathbb{1}_4 - 2|\psi(ij)\rangle\langle\psi(ij)|. \tag{71}$$

As an example, for $i = j = 1$, we have the Yang–Baxter gate $P \equiv R(11)$, given by

$$P = \begin{pmatrix} 1 & 0 & 0 & 0 \\ 0 & 0 & 1 & 0 \\ 0 & 1 & 0 & 0 \\ 0 & 0 & 0 & 1 \end{pmatrix} \tag{72}$$

which is the Permutation gate (or the Swap gate) P in quantum computation [1]. Note that all of the special type I Yang–Baxter gates $R(ij)$ are permutation-like quantum gates satisfying $R(ij)R(ij) = \mathbb{1}_4$, and a further research has been done in Appendix B.

The special type I Yang–Baxter gate $R(ij)$ in the extended Temperley–Lieb diagrammatical approach is shown as

$R(ij) = \sum_{k,l=0}^{1}(1 - 2\delta_{i,k}\delta_{j,l})$ 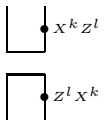

(73)

where the symbol δ denotes the Kronecker delta function. For example, the Yang–Baxter gate $P = R(11)$ has the extended Temperley–Lieb diagrammatical representation,

$P =$ 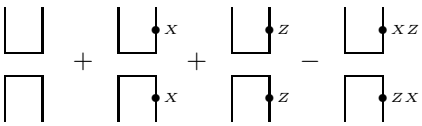

. (74)

Note that the special type I Yang–Baxter gate $R(ij)$ will not be applied to our study on teleportation-based quantum computation in Section 5, see Appendix B for a relevant interpretation. We present them here because they have a simplest realization in the extended Temperley–Lieb diagrammatical approach.

4.3 Special type II Yang–Baxter gate and its extended Temperley-Lieb diagrammatical representation

The special type II Yang–Baxter gates $B(\epsilon, \eta)$, or equivalently denoted as $B_{\epsilon,\eta}$, with $\epsilon = \pm 1$ and $\eta = \pm 1$, have the form

$$B(\epsilon, \eta) = \frac{1}{\sqrt{2}} \begin{pmatrix} 1 & 0 & 0 & \eta \\ 0 & 1 & \epsilon & 0 \\ 0 & -\epsilon & 1 & 0 \\ -\eta & 0 & 0 & 1 \end{pmatrix}, \tag{75}$$

which are derived in Appendix A.5.2 as examples for the Yang–Baxter gates generated by the Temperley–Lieb algebra. These four Yang–Baxter gates $B(\epsilon, \eta)$ are related to one another by the relations

$$B(\epsilon, \eta) = B^\dagger(-\epsilon, -\eta), \quad B(\epsilon, \eta) = PB(-\epsilon, \eta)P, \tag{76}$$

where P is the Permutation gate (72), and the inverse of such the Yang–Baxter gate $B(\epsilon,\eta)$ is related to itself with the aid of the Pauli Z gate, expressed as

$$B(\epsilon,\eta) = Z_1 B^{\dagger}(\epsilon,\eta) Z_1 = Z_2 B^{\dagger}(\epsilon,\eta) Z_2. \tag{77}$$

The special type II Yang–Baxter gates $B(\epsilon,\eta)$ are to be applied to our study on the reformulation of the teleportaiton-based quantum computation in Section 5, because they can generate the Bell states (5) from the product basis, see [19, 20, 21]. For example, when the parameters $\epsilon = 1$ and $\eta = 1$, we denote the Yang–Baxter gate B^5 as an abbreviation of the notation $B(1,1)$,

$$B = \frac{1}{\sqrt{2}} \begin{pmatrix} 1 & 0 & 0 & 1 \\ 0 & 1 & 1 & 0 \\ 0 & -1 & 1 & 0 \\ -1 & 0 & 0 & 1 \end{pmatrix} \tag{78}$$

which gives rise to all four Bell states from the product basis in the way

$$B \begin{pmatrix} |00\rangle \\ |01\rangle \\ |10\rangle \\ |11\rangle \end{pmatrix} = \begin{pmatrix} |\psi(01)\rangle \\ |\psi(11)\rangle \\ |\psi(10)\rangle \\ |\psi(00)\rangle \end{pmatrix}. \tag{79}$$

We can directly read the extended Temperley–Lieb configuration of the Yang–Baxter gate $B(\epsilon,\eta)$, shown as

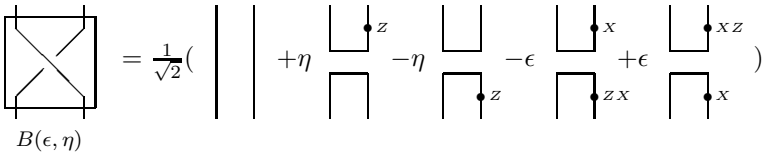

(80)

where the over-crossing diagram represents the braiding feature [15] of the Yang–Baxter gate $B(\epsilon,\eta)$ (75) and the box around it marks the feature that it can be regarded as a two-qubit quantum gate, and two parallel vertical lines represent the two-qubit identity gate (69). To maintain the diagrammatical representations consistent, the braiding configuration (the over-crossing configuration) has the same acting direction as the other extended Temperley–Lieb diagrammatic representations, namely, it is read from the bottom to the top.

5 The Yang–Baxter gate approach to teleportation-based quantum computation

In this section, we apply the special type II Yang–Baxter gates $B(\epsilon,\eta)$ (75), derived in Appendix A and presented in Section 4 with their associated extended Temperley–Lieb diagrammatical configurations (80), to teleportation-based quantum computation. First of all, such the special type II Yang–Baxter gates $B(\epsilon,\eta)$ are found to be a type of examples for the Bell transform defined in [13], where teleportation-based quantum computation using the Bell transform has been explored in detail. Note that the Yang–Baxter gate approach to teleportation-based quantum computation admits an interpretation in the extended Temperley–Lieb diagrammatical approach, see Section 6.

[5]The Yang–Baxter gate B in this paper is denoted as the Yang–Baxter gate B' in the authors' another paper [13].

Operation	Input	Output
$B_{-1,1}$	X_1	X_1
	X_2	X_1Z_2
	Z_1	$-Y_1Y_2$
	Z_2	$-X_1X_2$
$B_{1,-1}$	X_1	X_1
	X_2	$-X_1Z_2$
	Z_1	Y_1Y_2
	Z_2	X_1X_2
$B_{1,1}$	X_1	Z_1X_2
	X_2	X_2
	Z_1	$-X_1X_2$
	Z_2	$-Y_1Y_2$
$B_{-1,-1}$	X_1	$-Z_1X_2$
	X_2	X_2
	Z_1	X_1X_2
	Z_2	Y_1Y_2

Table 1: Transformation properties of elements of the Pauli group $\mathcal{P}_2$ under conjugation by the Yang–Baxter gates $B_{\epsilon,\eta}$ (75) where the variables ϵ and η are relabeled as subscripts.

5.1 The Yang–Baxter gate $B(\epsilon,\eta)$ as the Bell transform and Clifford gate

We recognize the special type II Yang–Baxter gate $B(\epsilon,\eta)$ (75) as the Bell transform [13], and especially verify them as Clifford gates [1, 28] in three equivalent approaches.

A type of the Bell transform [13] is defined as a two-qubit quantum gate capable of generating the four Bell states (5) from the product states modulo global phase factors. For examples, the special type II Yang–Baxter gates $B(\epsilon,\eta)$, denoted by $B_{\epsilon,\eta}$ in this section, are the Bell transform because they produce the Bell states in the way,

$$B_{-1,1}|ij\rangle = (-1)^{i\cdot(j+1)}|\psi(i+j,j+1)\rangle, \tag{81}$$

$$B_{1,-1}|ij\rangle = (-1)^{i\cdot j}|\psi(i+j,j)\rangle, \tag{82}$$

$$B_{1,1}|ij\rangle = |\psi(i+j,i+1)\rangle, \tag{83}$$

$$B_{-1,-1}|ij\rangle = (-1)^{i}|\psi(i+j,i)\rangle, \tag{84}$$

in which the addition is the binary addition and the multiplication is the logical AND operation. Obviously, the global phase factors of such the Bell states generated by the $B_{\epsilon,\eta}$ gates are ± 1, so the special type II Yang–Baxter gates $B_{\epsilon,\eta}$ are Clifford gates [1, 28], because the global phase factors associated with Clifford gates are allowed to be only ± 1, $\pm i$ [13].

According to discussed in Subsubsection 2.3.2, the fact that the special type II Yang–Baxter gates $B_{\epsilon,\eta}$ are Clifford gates is crucial in the fault-tolerant construction of universal quantum gate set using quantum teleportation in the following subsections. We will verify the $B_{\epsilon,\eta}$ gates as Clifford gates in another two ways. A Clifford gate can be expressed as a tensor product of elementary Clifford gates, namely the Hadamard gate H (10), the phase gate S (18) and the $CNOT$ gate (12), so we reformulate the $B_{-1,1}$ gate as

$$B_{-1,1} = CNOT_{21}(\mathbb{1}_2 \otimes ZH)CNOT_{21}, \tag{85}$$

with $Z = S^2$. With the algebraic relations (76) among the $B_{\epsilon,\eta}$ gates, for examples, the $B_{1,-1}$ gate is the inverse of the $B_{-1,1}$ gate and the $B_{1,1}$ gate is the conjugation of the $B_{-1,1}$ gate under the Permutation gate, we can decompose all the $B_{\epsilon,\eta}$ gates as tensor products of elementary Clifford gates. Besides such the decompositions, the Clifford gates $B_{\epsilon,\eta}$ are verified to preserve the properties of Pauli group $\mathcal{P}_2$ generated by X_1, X_2 and Z_1, Z_2 under conjugation by the Yang–Baxter gates $B_{\epsilon,\eta}$ (75), see Table 1. Note that the results in Table 1 will be exploited in the study of the Yang–Baxter gate approach to teleportation-based quantum computation.

ϵ	η	$p_{\epsilon,\eta}$	$p'_{\epsilon,\eta}$	$a_{\epsilon,\eta}$	$b_{\epsilon,\eta}$
-1	1	$j\cdot(j+k+l)$	$i\cdot j+(k+l)\cdot(j+l+1)$	$j+l+1$	$i+j+k+l$
1	-1	$k\cdot l+(k+l)\cdot(j+l+1)$	$k\cdot l+(j+1)\cdot(i+k+l)$		
1	1	$i\cdot j+(k+l)\cdot(i+k+1)$	$i\cdot(i+k+l)$	$i+k+1$	$i+j+k+l$
-1	-1	$k\cdot l+(i+1)\cdot(j+k+l)$	$l+i\cdot(k+l)$		

Table 2: The indices $p_{\epsilon,\eta}$, $p'_{\epsilon,\eta}$, $a_{\epsilon,\eta}$ and $b_{\epsilon,\eta}$ for both the local unitary gate $W_{\epsilon,\eta}$ (88) in the teleportation equation (87) and the local unitary gate $W'_{\epsilon,\eta}$ (90) in the teleportation equation (89). The multiplication $\cdot$ is a logical AND operation and the addition $+$ is a binary addition.

5.2 Quantum teleportation circuit using the Yang–Baxter gate

The essential ingredient in quantum teleportation circuit model is the teleportation operator introduced in [13] which is the tensor product of the identity operator, the Bell transform and its inverse. Here, the special type II Yang–Baxter gates $B_{\epsilon,\eta}$ are the Bell transform, so we make use of a similar type of the teleportation operators

$$(B_{\epsilon,\eta}\otimes\mathbb{1}_2)(\mathbb{1}_2\otimes B_{\epsilon,\eta})\quad\text{or}\quad(\mathbb{1}_2\otimes B_{\epsilon,\eta})(B_{\epsilon,\eta}\otimes\mathbb{1}_2) \tag{86}$$

to act on the product state $|\alpha\rangle|kl\rangle$ or $|kl\rangle|\alpha\rangle$ respectively. They give rise to the type of the teleportation equation

$$(B_{\epsilon,\eta}\otimes\mathbb{1}_2)(\mathbb{1}_2\otimes B_{\epsilon,\eta})(|\alpha\rangle\otimes|kl\rangle)=\frac{1}{2}\sum_{i,j=0}^{1}|ij\rangle W_{\epsilon,\eta}|\alpha\rangle, \tag{87}$$

which is associated with the teleportation equation (6) with the local single-qubit gate

$$W_{\epsilon,\eta}=(-1)^{p_{\epsilon,\eta}}Z^{a_{\epsilon,\eta}}X^{b_{\epsilon,\eta}}, \tag{88}$$

to represent the protocol of transmitting an unknown qubit $|\alpha\rangle$ from Alice to Bob, and the other type of the teleportation equation

$$(\mathbb{1}_2\otimes B_{\epsilon,\eta})(B_{\epsilon,\eta}\otimes\mathbb{1}_2)(|kl\rangle\otimes|\alpha\rangle)=\frac{1}{2}\sum_{i,j=0}^{1}W'_{\epsilon,\eta}|\alpha\rangle|ij\rangle, \tag{89}$$

which is related to the teleportation equation (9) with the local single-qubit gate

$$W'_{\epsilon,\eta}=(-1)^{p'_{\epsilon,\eta}}Z^{a_{\epsilon,\eta}}X^{b_{\epsilon,\eta}}, \tag{90}$$

to represent the protocol of transmitting an unknown qubit $|\alpha\rangle$ from Bob to Alice, where the explicit expressions for the indices $p_{\epsilon,\eta}$, $p'_{\epsilon,\eta}$, $a_{\epsilon,\eta}$ and $b_{\epsilon,\eta}$ in both single-qubit gates $W_{\epsilon,\eta}$ (88) and $W'_{\epsilon,\eta}$ (90) are shown up in Table 2. Note that the local single-qubit gates $W_{\epsilon,\eta}$ (88) and $W'_{\epsilon,\eta}$ (90) are almost the same except the global phase factors.

Based on the above teleportation equations (87) or (89) using the special type II Yang–Baxter gates $B_{\epsilon,\eta}$, we continue to perform single-qubit measurements, classical communication and local unitary corrections to complete the entire quantum teleportation protocol. For example, the quantum teleportation circuit model associated with the teleportation equation (87) is drawn in Figure 5, where the braiding configuration (80) of the Yang–Baxter gate $B_{\epsilon,\eta}$ has been applied. About the teleportation circuit model in Figure 5, the special type II Yang–Baxter gate $B(\epsilon,\eta)$ acting on the product state $|kl\rangle$ gives the prepared Bell states, and the same Yang–Baxter gate $B(\epsilon,\eta)$ followed by two single-qubit measurements works as the Bell measurements.

Note that the inverse of the Yang–Baxter gate $B(\epsilon,\eta)$, denoted by $B^{\dagger}(\epsilon,\eta)$, is related to itself with the algebraic relation (77). In other words, the inverse of the Yang–Baxter gate $B(\epsilon,\eta)$

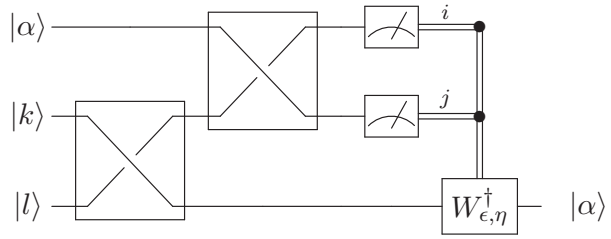

Figure 5: Quantum circuit of teleportation corresponding to the teleportation equation (87). The Yang–Baxter gate $B(\epsilon, \eta)$ (75) is represented by a braiding configuration inside a two-qubit gate box. In accordance with the conventional rules of the quantum circuit diagram in Figure 1, the braiding configuration (80) of the Yang–Baxter gate $B(\epsilon, \eta)$ has been adjusted in the left-to-right direction from the original down-to-up direction. The left lower braiding on the product state $|kl\rangle$ is used to generate the prepared Bell states, and the right higher braiding followed with single-qubit state measurements works as the Bell measurements. The present quantum circuit model is essentially equivalent with the one in Figure 1, while the superficial differences between them are due to the fact that we are using various of presentations of both Bell states and Bell measurements.

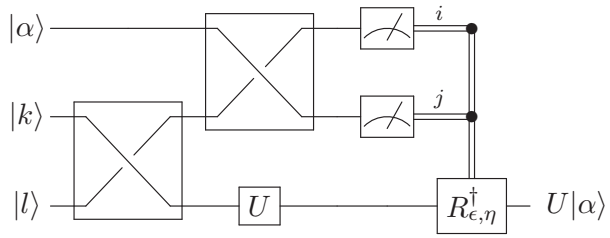

Figure 6: Quantum circuit for the fault-tolerant construction of a single-qubit gate U in the Yang–Baxter gate approach to teleportation-based quantum computation, associated with the teleportation equation (92), and it is equivalent with the quantum circuit in Figure 2.

is still the Bell transform [13]. Hence in terms of the inverse of the Yang–Baxter gate $B(\epsilon, \eta)$, the teleportation operators (86) can be reformulated as the same type of the teleportation operators used in [13] where the inverse of the Bell transform [13] with single-qubit measurements represents the Bell measurements.

5.3 Teleportation-based quantum computation using the Yang–Baxter gate

Under the guidance of the fault-tolerant construction of single-qubit gates in Subsubsection 2.3.3, we prepare the three-qubit quantum state in the the Yang–Baxter gate approach, expressed as

$$(\mathbb{1}_2 \otimes \mathbb{1}_2 \otimes U)(\mathbb{1}_2 \otimes B_{\epsilon,\eta})(|\alpha\rangle \otimes |kl\rangle) \tag{91}$$

with the single-qubit gate U acting on the Bell states, which are generated by the special type II Yang–Baxter gate $B(\epsilon, \eta)$ on the product basis $|kl\rangle$, and then apply the Yang–Baxter gate $B(\epsilon, \eta)$ on the first and second qubits to derive the teleportation equation

$$(B_{\epsilon,\eta} \otimes \mathbb{1}_2)(\mathbb{1}_2 \otimes \mathbb{1}_2 \otimes U)(\mathbb{1}_2 \otimes B_{\epsilon,\eta})(|\alpha\rangle \otimes |kl\rangle) = \frac{1}{2} \sum_{i,j=0}^{1} |ij\rangle R_{\epsilon,\eta} U|\alpha\rangle, \tag{92}$$

ϵ	η	$Q_{\epsilon,\eta}$	$P_{\epsilon,\eta}$
-1	1	$(-1)^{p_1+a_1}Y^{a_1}X^{b_1+b_2+a_2}$	$(-1)^{p_2'+a_2}Y^{a_1}X^{a_2}Z^{b_2}$
1	-1	$(-1)^{p_1}Y^{a_1}X^{b_1+b_2+a_2}$	$(-1)^{p_2'+b_2}Y^{a_1}X^{a_2}Z^{b_2}$
1	1	$(-1)^{p_1+a_1}X^{a_1}Z^{b_1}Y^{a_2}$	$(-1)^{p_2'+a_2}X^{a_1+b_1}Y^{a_2}X^{b_2}$
-1	-1	$(-1)^{p_1+b_1}X^{a_1}Z^{b_1}Y^{a_2}$	$(-1)^{p_2'}X^{a_1+b_1}Y^{a_2}X^{b_2}$

Table 3: The $Q_{\epsilon,\eta}$ and $P_{\epsilon,\eta}$ gates in the teleportation equation (95). For simplicity, the subscripts ϵ and η of p, p', a and b, are omitted in the present table without confusion. The parameters p_1, p_1', a_1 and b_1 depend on the parameters i_1, j_1, k_1 and l_1, and are calculated by the formulas in Table 2, while the parameters p_2, p_2', a_2 and b_2 depend on the parameters i_2, j_2, k_2 and l_2, and are calculated by the formulas in Table 2.

which is associated with the teleportation equation (20), with $R_{\epsilon,\eta} = UW_{\epsilon,\eta}U^\dagger$, the single-qubit gate $W_{\epsilon,\eta}$ defined in (88).

For example, when the single-qubit gate U is the Hadamard gate H (10) and $\pi/8$ gate T (11), the corresponding single-qubit gates $R_{\epsilon,\eta}$ have the form respectively,

$$R_{\epsilon,\eta}(H) = (-1)^{p_{\epsilon,\eta}} X^{a_{\epsilon,\eta}} Z^{b_{\epsilon,\eta}}, \quad R_{\epsilon,\eta}(T) = (-1)^{p_{\epsilon,\eta}} Z^{a_{\epsilon,\eta}} \left(\frac{X - \sqrt{-1}Y}{\sqrt{2}}\right)^{b_{\epsilon,\eta}}, \tag{93}$$

where the indices $p_{\epsilon,\eta}$, $a_{\epsilon,\eta}$ and $b_{\epsilon,\eta}$ are those in Table 2. We can compare these results with their counterparts obtained in Subsubsection 2.3.3, such as (21). Note that the $R_{\epsilon,\eta}(H)$ gates are the Pauli gates with the global phase factors, whereas the $R_{\epsilon,\eta}(T)$ gates are the Clifford gates.

Combining the teleportation equation (92) with both two single-qubit measurements and the local unitary correction operator $R_{\epsilon,\eta}^\dagger$, the quantum circuit model for the fault-tolerant construction of the single-qubit gate U in the Yang–Baxter gate approach is presented in Figure 6, which can be compared with the quantum circuit model in Figure 2.

In accordance with the fault-tolerant construction of a two-qubit Clifford gate in Subsubsection 2.3.4, we perform the fault-tolerant construction of the special type II Yang–Baxter gate $B(\epsilon,\eta)$ (75) in the following steps. Firstly, we prepare the four-qubit entangled state in the Yang–Baxter gate approach as

$$(\mathbb{1}_2 \otimes B_{\epsilon,\eta} \otimes \mathbb{1}_2)(B_{\epsilon,\eta} \otimes B_{\epsilon,\eta})(|k_1 l_1\rangle \otimes |k_2 l_2\rangle). \tag{94}$$

Secondly, we perform two Bell measurements respectively via two Yang–Baxter gates $B(\epsilon,\eta)$ followed by product-basis measurements, so that we have the teleportation equation

$$\begin{aligned} & (B_{\epsilon,\eta} \otimes B_{\epsilon,\eta} \otimes B_{\epsilon,\eta})(\mathbb{1}_2 \otimes B_{\epsilon,\eta} \otimes B_{\epsilon,\eta} \otimes \mathbb{1}_2)(|\alpha\rangle \otimes |k_1 l_1\rangle \otimes |k_2 l_2\rangle \otimes |\beta\rangle) \\ = \; & \frac{1}{4} \sum_{i_1,j_1=0}^{1} \sum_{i_2,j_2=0}^{1} (\mathbb{1}_4 \otimes Q_{\epsilon,\eta} \otimes P_{\epsilon,\eta} \otimes \mathbb{1}_4)(|i_1 j_1\rangle \otimes B_{\epsilon,\eta}|\alpha\beta\rangle \otimes |i_2 j_2\rangle), \end{aligned} \tag{95}$$

which is related to the teleportation equation (23) and has the quantum circuit in Figure 7. The single-qubit gates $Q_{\epsilon,\eta}$ and $P_{\epsilon,\eta}$ are calculated by the formula

$$Q_{\epsilon,\eta} \otimes P_{\epsilon,\eta} = B_{\epsilon,\eta}(W_{\epsilon,\eta} \otimes W'_{\epsilon,\eta})B_{-\epsilon,-\eta}, \tag{96}$$

in which $W_{\epsilon,\eta}$ is defined in (87) and depends on the indices i_1, j_1, and $W'_{\epsilon,\eta}$ is defined in (89) and depends on the indices i_2, j_2, and the explicit expressions of $Q_{\epsilon,\eta}$ and $P_{\epsilon,\eta}$ are listed in Table 3.

5.4 Special example: $\epsilon = 1, \eta = 1$ and $|kl\rangle = |11\rangle$

For readers' convenience, we make a brief summary on the results in the Yang–Baxter gate approach to the teleportation-based quantum computation using the Yang–Baxter gate B (78), which

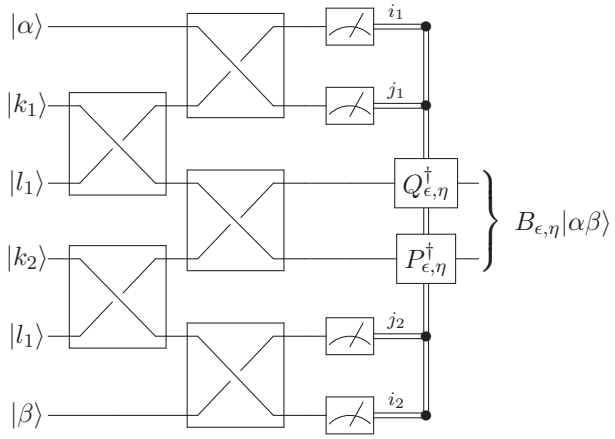

Figure 7: Quantum circuit for the fault-tolerant construction of the two-qubit gate $B_{\epsilon,\eta}$ (75) in the Yang–Baxter gate approach to teleportation-based quantum computation, associated with the teleportation equation (95), and it is equivalent with the quantum circuit in Figure 3. Explicit expressions for single-qubit gates $Q^\dagger_{\epsilon,\eta}$ and $P^\dagger_{\epsilon,\eta}$ are shown up in Table 3.

is the $B_{\epsilon,\eta}$ gate (75) of $\epsilon = 1, \eta = 1$. To further simplify the calculation results without losing any significant physical meaning, we choose the product state $|kl\rangle = |11\rangle$ in the state preparation. Note that the Yang–Baxter gate B (78) acting on the state $|11\rangle$ gives rise to the EPR state (3).

First, the teleportation equation associated with the teleportation operator $(B \otimes \mathbb{1}_2)(\mathbb{1}_2 \otimes B)$ on the product state $|\alpha\rangle \otimes |11\rangle$ has the form

$$(B \otimes \mathbb{1}_2)(\mathbb{1}_2 \otimes B)(|\alpha\rangle \otimes |11\rangle) = \frac{1}{2} \sum_{i,j=0}^{1} |ij\rangle W_B |\alpha\rangle, \tag{97}$$

with the single-qubit gate W_B given by

$$W_B = (-1)^{i \cdot j} Z^i X^{i+j}, \tag{98}$$

which is a special case of the teleportation equation (87). Similarly, the teleportation equation, as a special example of (89), is obtained to be

$$(\mathbb{1}_2 \otimes B)(B \otimes \mathbb{1}_2)(|11\rangle \otimes |\alpha\rangle) = \frac{1}{2} \sum_{i,j=0}^{1} W_B^T |\alpha\rangle |ij\rangle, \tag{99}$$

where W_B^T is the matrix transpose of W_B (98).

Second, the teleportation equation associated with the fault-tolerant construction of the single-qubit gate U has the form

$$(B \otimes \mathbb{1}_2)(\mathbb{1}_2 \otimes \mathbb{1}_2 \otimes U)(\mathbb{1}_2 \otimes B)(|\alpha\rangle \otimes |11\rangle) = \frac{1}{2} \sum_{i,j=0}^{1} |ij\rangle R_B\, U |\alpha\rangle, \tag{100}$$

with $R_B = U W_B U^\dagger$, the W_B gate defined in (98), which is a special example of the teleportation equation (92). As the single-qubit gate U is the Hadamard gate H (10) and the $\pi/8$ gate T (11) respectively, the local unitary gate R_B has the explicit forms

$$R_B(H) = (-1)^{i \cdot j} X^i Z^{i+j}, \quad R_B(T) = (-1)^{i \cdot j} Z^i \left(\frac{X - \sqrt{-1}Y}{\sqrt{2}} \right)^{i+j}. \tag{101}$$

Third, the teleportation equation associated with the fault-tolerant construction of the Yang–Baxter gate B, as a special case of (95), has the form

$$\begin{aligned}&(B\otimes B\otimes B)(\mathbb{1}_2\otimes B\otimes B\otimes \mathbb{1}_2)(|\alpha\rangle\otimes|11\rangle\otimes|11\rangle\otimes|\beta\rangle)\\ =\;&\frac{1}{4}\sum_{i_1,j_1=0}^{1}\sum_{i_2,j_2=0}^{1}(\mathbb{1}_4\otimes Q_B\otimes P_B\otimes \mathbb{1}_4)(|i_1j_1\rangle\otimes B|\alpha\beta\rangle\otimes|i_2j_2\rangle),\end{aligned}\tag{102}$$

with the single-qubit gates Q_B and P_B calculated by

$$Q_B\otimes P_B = B(W_B\otimes W_B^T)B^\dagger,\tag{103}$$

where W_B depends on the parameters i_1, j_1 and W_B^T depends on the parameters i_2, j_2. The explicit formalisms of Q_B and P_B are expressed as

$$Q_B=(-1)^{i_1\cdot(j_1+1)}X^{i_1}Z^{i_1+j_1}Y^{i_2},\quad P_B=X^{j_1}Y^{i_2}X^{i_2+j_2}\tag{104}$$

which can be derived with Table 3 by picking up the third row of $\epsilon=1,\eta=1$, and setting $k_1=l_1=k_2=l_2=1$.

Note that the key reason that the results in this subsection are presented is that they are to be explained in the extended Temperley–Lieb diagrammatical approach in Section 6.

6 Relationship between the extended Temperley–Lieb diagrammatical approach and the Yang–Baxter gate approach

So far, we study the two approaches to teleportation-based quantum computation: the one is the extended Temperley–Lieb diagrammatical approach in Section 3, and the other is the Yang–Baxter gate approach in Section 5. In this section, we are in a position to consider the relationship between these two approaches. With the extended Temperley–Lieb configuration (80) of the special type II Yang–Baxter gate $B(\epsilon,\eta)$ (75) in Section 4, we are able to recast all the algebraic results of the Yang–Baxter gate approach in Section 5 into the topological diagrammatical configurations, which are found to be those in the extended Temperley–Lieb diagrammatical approach in Section 3. In the following discussion, we concentrate on the Yang–Baxter gate B (78) as an example for the special type II Yang–Baxter gate $B(\epsilon,\eta)$ with $\epsilon=\eta=1$.

6.1 The product basis and the Bell basis

The Yang–Baxter gate approach to teleportation-based quantum computation in Section 5 is based on the observation that the Bell states (5) can be replaced by the Yang–Baxter gate acting on the product states and the Bell measurements can be substituted by the Yang–Baxter gate followed with product-basis measurements. Hence, the first thing that we are going to do is to describe the product basis and the Bell basis in the extended Temperley–Lieb diagrammatical approach.

With the definition of the Bell basis (5), it is easy to formulate the two-qubit product basis in terms of the Bell basis, so the two-qubit product states have the extended Temperley–Lieb diagrammatical configurations respectively expressed as

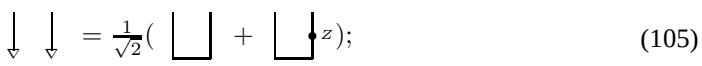

(105)

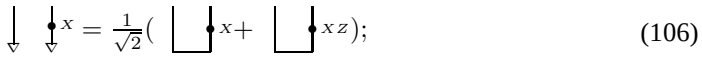

(106)

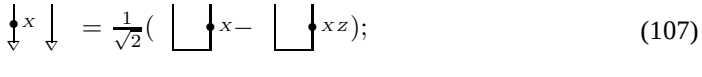

(107)

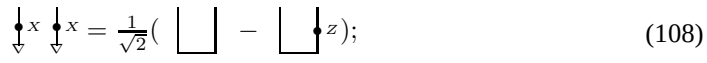

(108)

where the vertical line with ∇ stands for the state $|0\rangle$ and naturally the one with the Pauli X gate stands for the state $|1\rangle$. And the adjoint of the above algebraic relations (105)-(108) have the extended Temperley–Lieb diagrammatical configurations respectively as

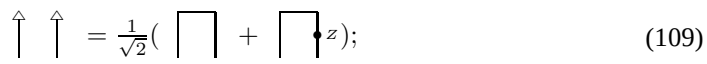

(109)

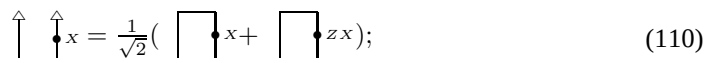

(110)

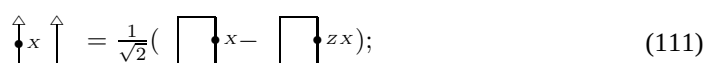

(111)

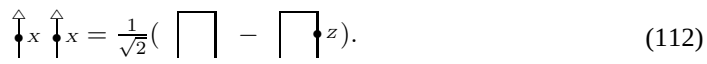

(112)

Now we study the action of the Yang–Baxter gate B (78) on the product state $|ij\rangle$ in the extended Temperley–Lieb diagrammatical approach. The extended Temperley–Lieb configuration of the Yang–Baxter gate B (78), has the form

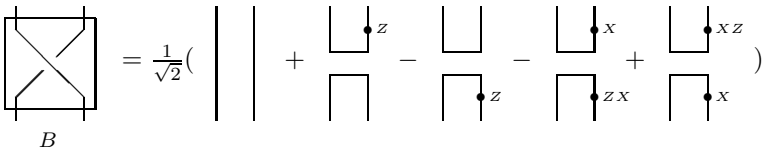

(113)

which is directly obtained from (80) by setting $\epsilon = 1, \eta = 1$. With the extended Temperley–Lieb diagrammatical rules [18] that assign a normalization factor 1 to a loop configuration and assign a normalized trace of single-qubit gates to a loop with the action of associated single-qubit gates, for example, we apply the Yang–Baxter gate B on the product state $|11\rangle$, namely calculate $B|11\rangle$ in the diagrammatical approach,

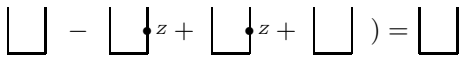

(114)

which is the cup representation of the EPR state $|\Psi\rangle$, see (36). In the same manner, performing the Yang–Baxter gate B on the other product states, we attain the extended Temperley–Lieb configurations of the other Bell states, summarized in

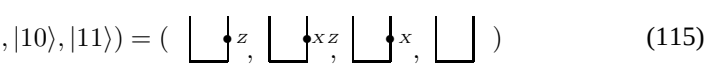

(115)

which allows a more concise expression as

(116)

with the single-qubit gate $V_{kl} = X^{k+l}Z^{k+1}$. Note that the diagrammatical representation (116) is associated with the algebraic relation (83).

The Yang–Baxter gate B followed with the product-state measurements has the algebraic form $|ij\rangle\langle ij|B$. For simplicity, we neglect the post-measurement state $|ij\rangle$, and only calculate

$\langle ij|B$ in the extended Temperley–Lieb diagrammatical approach. For example, the quantum state $\langle 00|B$ is calculated in the way

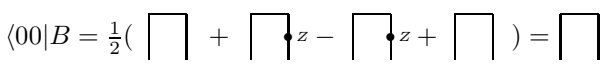

(117)

which is the cap representation of the EPR state $|\Psi\rangle$, see (37). After calculating the other cases, it turns out that the state $\langle ij|B$ has the representation,

(118)

with the single-qubit gate $U_{ij} = (-1)^i Z^i X^{i+j}$. Note that the diagrammatical representation (118) is associated with the adjoint of the algebraic relation (84) in which the Bell transform $B_{-1,-1}$ is the inverse of the Bell transform B.

6.2 Teleportation-based quantum computation

Let us derive the extended Temperley–Lieb configurations in Section 3 respectively from the Yang–Baxter gate approach to teleportation-based quantum computation in Section 5.

The topological representation of quantum teleportation, such as (42), can be regarded as the diagrammatical representation of a matrix element of the teleportation equation (97) using the Yang–Baxter gate B. With the cup state (114) generated by $B|11\rangle$ and the cap state (118) generated by $\langle ij|B$, the teleportation operator $(B \otimes \mathbb{1}_2)(\mathbb{1} \otimes B)$ has the matrix element as

$(\langle ij| \otimes \mathbb{1}_2)(B \otimes \mathbb{1}_2)(\mathbb{1}_2 \otimes B)|\alpha\rangle \otimes |11\rangle =$

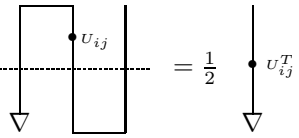

(119)

in which the diagrammatical part below the dashed line denotes the prepared state $|\alpha\rangle \otimes |\Psi\rangle$ and the part above the dashed line denotes the Bell measurement labeled by the single-qubit gate U_{ij} in (118). The transpose of U_{ij} is the local unitary gate W_B (98), namely, $U_{ij}^T = W_B$. Note that the post-measurement state $B^\dagger|ij\rangle$ is neglected for simplicity. As another example, the topological configuration (43) of the chained teleportation is obtained in the Yang–Baxter gate approach,

$({}_{1234}\langle 0000| \otimes \mathbb{1}_2)B_{12}B_{34}B_{23}B_{45}|\alpha\rangle_1 \otimes |1111\rangle_{2345} =$

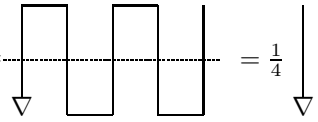

(120)

where $B|11\rangle$ denotes the cup state (114) and $\langle 00|B$ denotes the cap state (117) and the symbol B_{ij} means that the Yang–Baxter gate B is acting on both the i-th and j-th qubits.

The topological configuration (44) for the fault-tolerant construction of the single-qubit gate U in teleportation-based quantum computation is associated with the matrix element of the teleportation equation (100),

$(\langle ij| \otimes \mathbb{1}_2)(B \otimes \mathbb{1}_2)(\mathbb{1}_2 \otimes \mathbb{1}_2 \otimes U)(\mathbb{1} \otimes B)|\alpha\rangle \otimes |11\rangle =$

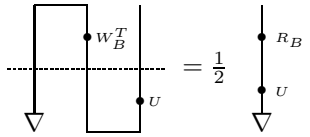

(121)

with $R_B = UW_BU^\dagger$, where the single-qubit gate U_{ij} in (118) is denoted as the W_B^T gate to avoid a possible notational confusion. Furthermore, the algebraic counterpart of the topological

configuration (45) of the fault-tolerant construction of the Yang–Baxter gate B which is a two-qubit Clifford gate, is the matrix element of the teleportation equation (102), expressed as

$$(\langle i_1 j_1| \otimes \mathbb{1}_2 \otimes \mathbb{1}_2 \otimes \langle i_2 j_2|)(B \otimes B \otimes B)(\mathbb{1}_2 \otimes B \otimes B \otimes \mathbb{1}_2)(|\alpha\rangle \otimes |11\rangle \otimes |11\rangle \otimes |\beta\rangle)$$

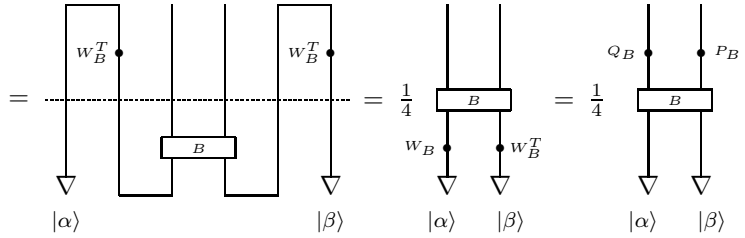

(122)

where the single-qubit gate W_B^T acting on the second qubit depends on the indices i_1, j_1 and the single-qubit gate W_B^T on the sixth qubit depends on the indices i_2, j_2 and the single-qubit gates Q_B and P_B are derived by the formula (103).

6.3 The teleportation operator and the teleportation equation

As shown up in Section 5, the teleportation operator (86) plays the key role in the Yang–Baxter gate approach to teleportation-based quantum computation, and it is accompanied with both the product state preparation and the product state measurement to perform the teleportation protocol. In this subsection, we study the diagrammatical representation of the teleportation operator $(B \otimes \mathbb{1}_2)(\mathbb{1}_2 \otimes B)$ by combining the configuration of the product basis with the extended Temperley–Lieb diagrammatical approach, and from such the diagrammatical representation, we can easily derive the teleportation equation of the type (97).

With the extended Temperley–Lieb configuration (69) of the two-qubit identity gate, the Yang–Baxter gate B (78) has the configuration

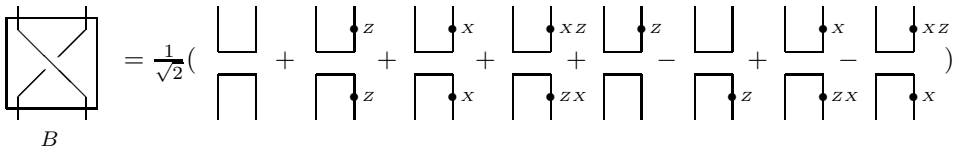

(123)

which is equivalent to a special case of the extended Temperley–Lieb configuration (172). Applying the algebraic relations (109)-(112) on the configuration (123), the Yang–Baxter gate B (78) has its compact diagrammatical representation

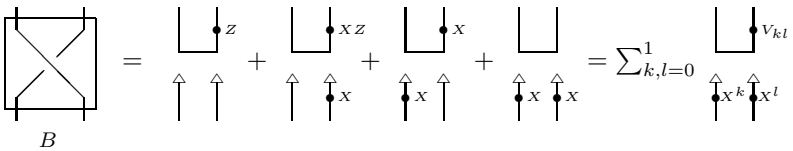

(124)

where the single-qubit gate V_{kl} is defined in (116), and the associated algebraic formulation of such the configuration (124) is expressed as

$$B = \sum_{k,l=0}^{1} |\Psi_{V_{kl}}\rangle\langle kl| = \sum_{k,l=0}^{1} |\psi(k+l, k+1)\rangle\langle kl|, \tag{125}$$

with $|\Psi_{V_{kl}}\rangle$ defined in (19), which is obviously the defining relation (83) of the Bell transform B.

	$i=0, j=0$	$i=0, j=1$	$i=1, j=0$	$i=1, j=1$
$k=0, l=0$	Z	$-XZ$	X	$-\mathbb{1}_2$
$k=0, l=1$	XZ	$-Z$	$\mathbb{1}_2$	$-X$
$k=1, l=0$	X	$\mathbb{1}_2$	$-Z$	XZ
$k=1, l=1$	$\mathbb{1}_2$	X	$-XZ$	$-Z$

Table 4: The single-qubit gate $W_{1,1}$ (130) in both the algebraic expansion (131) of the teleportation operator $(B \otimes \mathbb{1}_2)(\mathbb{1}_2 \otimes B)$ and the teleportation equation (132).

On the other hand, applying the algebraic relations (105)-(108) on the configuration (123) of the Yang–Baxter gate B gives rise to its another compact configuration

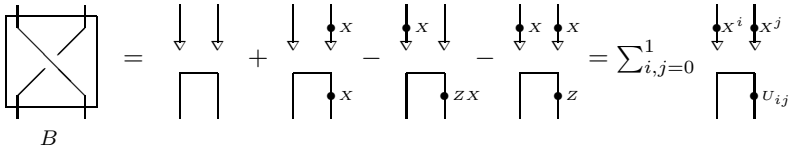

(126)

where the single-qubit gate U_{ij} is defined in (118), and the associated algebraic expression is

$$B = \sum_{i,j=0}^{1} |ij\rangle\langle\Psi_{U_{ij}}| = \sum_{i,j=0}^{1} (-1)^j |ij\rangle\langle\psi(i+j,i)|, \tag{127}$$

with $|\Psi_{U_{ij}}\rangle$ defined in (19), from which the Yang–Baxter gate B can be also viewed as the inverse of the Bell transform from the Bell basis to the product basis. Note that in [13] the inverse of the Bell transform with the product basis measurement is regarded as the Bell measurement, hence the Yang–Baxter gate B acted by the product state can be viewed as the Bell measurement.

In the algebraic approach, the teleportation operator $(B \otimes \mathbb{1}_2)(\mathbb{1}_2 \otimes B)$ has the form

$$(B \otimes \mathbb{1}_2)(\mathbb{1}_2 \otimes B) = \sum_{i,j,k,l=0}^{1} (|ij\rangle\langle\Psi_{U_{ij}}| \otimes \mathbb{1}_2)(\mathbb{1}_2 \otimes |\Psi_{V_{kl}}\rangle\langle kl|) \tag{128}$$

where the left Yang–Baxter gate B represents the inverse of the Bell transform (127) with the configuration (126) and the right one denotes the Bell transform (125) with the configuration (124). Therefore, such the teleportation operator is calculated in the diagrammatical approach,

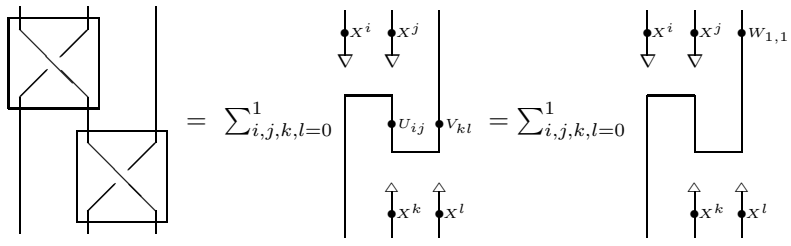

(129)

where the single-qubit gate $W_{1,1} = V_{kl} U_{ij}^T$ expressed as

$$W_{1,1} = (-1)^{i\cdot j + (k+l)\cdot(i+k+1)} Z^{i+k+1} X^{i+j+k+l}, \tag{130}$$

can be also calculated from the formula (88) by setting $\epsilon = \eta = 1$. See Table 4 for the explicit expressions of the single-qubit gate $W_{1,1}$.

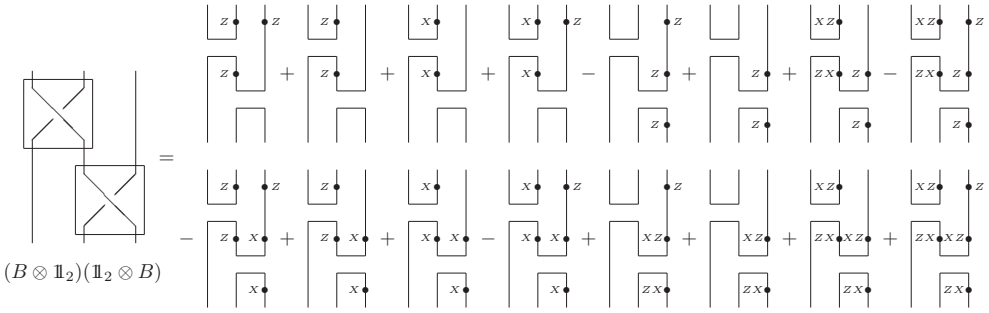

Figure 8: The extended Temperley–Lieb configuration of the teleportation operator $(B\otimes\mathbb{1}_2)(\mathbb{1}_2\otimes B)$ from the viewpoint of Bell measurements. The result is derived by directly applying the extended Temperley–Lieb configuration (123) of the Yang–Baxter gate B (78). The vertical braiding configuration can be regarded as the one obtained by clockwise rotating the horizontal braiding configuration in the quantum circuit in Figure 5 by 90 degrees.

Furthermore, the algebraic counterpart of the diagram (129) can be rewritten as

$$(B \otimes \mathbb{1}_2)(\mathbb{1}_2 \otimes B) = \sum_{i,j,k,l=0}^{1} (|ij\rangle, W_{1,1}, \langle kl|), \tag{131}$$

with the algebraic notation $(|ij\rangle, W_{1,1}, \langle kl|)$ of the associated diagrammatical term, which gives rise to the teleportation equation

$$(B \otimes \mathbb{1}_2)(\mathbb{1}_2 \otimes B)|\alpha\rangle \otimes |kl\rangle = \frac{1}{2} \sum_{i,j=0}^{1} |ij\rangle W_{1,1}|\alpha\rangle, \tag{132}$$

with the teleportation equation (97) as its special example of $k = l = 1$. In this sense, each one of the total 16 teleportation configurations in the diagram (129) can be extracted by applying the product basis measurement on the teleportation operator $(B \otimes \mathbb{1}_2)(\mathbb{1}_2 \otimes B)$. In addition, Appendix E presents another equivalent method of deriving the algebraic structure (131) of the teleportation operator $(B \otimes \mathbb{1}_2)(\mathbb{1}_2 \otimes B)$.

6.4 The teleportation operator using Bell measurements

The extended Temperley–Lieb diagrammatical representation of the teleportation operator $(B \otimes \mathbb{1}_2)(\mathbb{1}_2 \otimes B)$ can be derived in a rather straightforward diagrammatical approach using the extended Temperley–Lieb configuration (123) of the Yang–Baxter gate B, and the result is shown up in Figure 8, which can be explicitly regarded as a kind of linear combination of 16 typical quantum teleportation processes using Bell measurements.

Although each one of these 16 diagrammatical teleportation terms in Figure 8 can be interpreted in the viewpoint of quantum teleportation, a linear combination of these diagrammatical terms can not be usually viewed as quantum teleportation. The reason is that the teleportation operator with the product basis measurement (instead of Bell measurements) gives rise to quantum teleportation, as discussed in Subsection 6.3. Note that the simplified version of Figure 8 is shown up in Figure 9.

Appendix E presents an algebraic method of deriving the extended Temperley–Lieb configuration in Figure 9, and it is obvious that the topological configuration in Figure 8 can be easily obtained from the configuration in Figure 9. It is worthwhile pointing out that such the extended Temperley–Lieb configurations in both the diagram (129) and Figure 9 come naturally from our

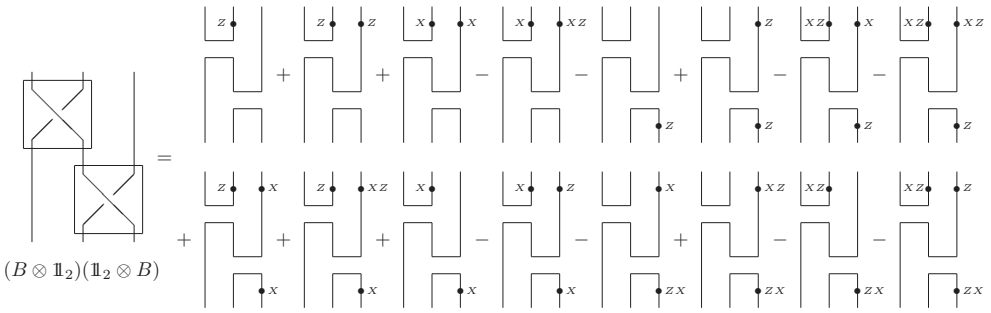

Figure 9: The extended Temperley–Lieb configuration of the teleportation operator $(B\otimes\mathbb{1}_2)(\mathbb{1}_2\otimes B)$ as a simplified version of the configuration in Figure 8.

topological and algebraic reformulations of teleportation-based quantum computation, whereas they are indeed unexpected if we consider the standard low dimensional topology [15]. Interested readers are invited to refer to Appendix A.

7 Concluding remarks

In this paper, we reformulate teleportation-based quantum computation [9, 10, 11] in both the extended Temperley–Lieb diagrammatical approach [17, 18] and the Yang–Baxter gate approach [19, 20, 21]. Such the two approaches can be respectively regarded as the topological aspect and algebraic aspect of a unified approach. On the other hand, through our research, the Yang–Baxter gate configuration (the braiding configuration) admits an equivalent description of a set of the extended Temperley–Lieb diagrammatical configurations, so we finally propose the extended Temperley–Lieb diagrammatical approach as an interesting topic for physicists in quantum information and computation. Our results show that the fact that quantum entanglement (or quantum non-locality) admits a kind of interpretation of topological entanglement (topological non-locality) takes the responsibility for topological features in teleportation-based quantum computation. Such topological features regard teleportation-based quantum circuit models as the two-dimensional topological deformations of the extended Temperley–Lieb diagrammatical configurations, and they greatly simplify the algebraic analysis in teleportation-based quantum computation. About further research, since teleportation-based quantum computation is an example for measurement-based quantum computation which includes the one-way quantum computation [27, 31] as another example, so we expect that the one-way quantum computation [27] can be also understood from both the extended Temperley–Lieb diagrammatical approach and the Yang–Baxter gate approach. Furthermore, if we consider the categorical description [32, 33, 34] of quantum teleportation, it is no doubt to obtain new insights on both our research results in this paper and categorical quantum information and computation. In addition, further research problems in mathematical physics are collected in Appendix A.6.

Acknowledgements

Yong Zhang is supported by the starting grant–273732 of Wuhan University.

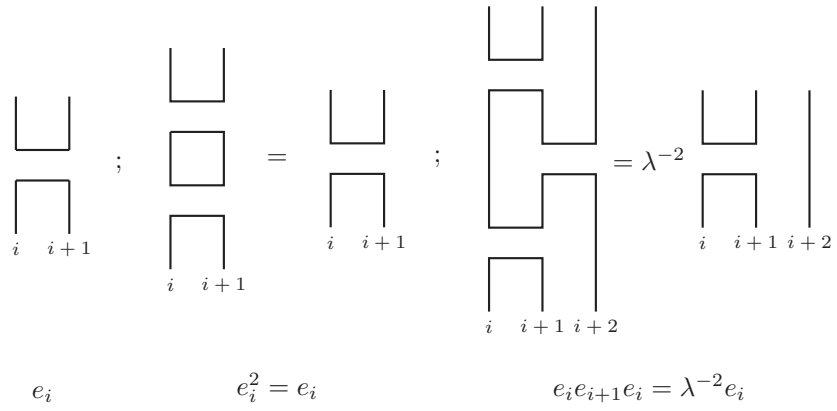

Figure 10: Diagrammatical representation of the algebraic relations defining the Temperley–Lieb algebra (133). The leftside diagram denotes the type of the idempotent e_i (134) acting on the i-th and $i+1$-th Hilbert spaces, where the vertical lines denoting an identity action on the 1-th, 2-th, $\cdots$, $i-1$-th, $i+2$-th, $\cdots$, n-th Hilbert spaces are neglected. The middle diagram denotes $e_i^2 = e_i$ in which the box (or the loop) represents the normalization factor 1 and can be thus omitted. The rightside diagram denotes $e_i e_{i+1} e_i = \lambda^{-2} e_i$, where the factor λ^{-2} is contributed by all the vanishing cups and caps in the topological straightening operation.

A The Yang–Baxter gate via the Temperley–Lieb algebra and its extended Temperley–Lieb diagrammatical representation

Recent years, non-trivial unitary solutions of the Yang–Baxter equation [16], called the Yang–Baxter gates [19, 20, 21], have been proposed in the study of quantum information and computation [1, 2]. Since the central topic of the present paper is about the application of the extended Temperley–Lieb diagrammatical approach to teleportation-based quantum computation [9, 10, 11], we study the construction of the Yang–Baxter gates using the Temperley–Lieb algebra [14, 15] in detail.

A.1 The Temperley–Lieb algebra and its diagrammatical representation

The Temperley–Lieb algebra [14, 15], denoted by $TL_n(\lambda)$, is generated by idempotents e_i which satisfy the algebraic relations:

$$\begin{aligned} e_i^2 &= e_i, \quad i = 1, \cdots, n-1; \\ e_i e_{i\pm 1} e_i &= \lambda^{-2} e_i; \\ e_i e_j &= e_j e_i, \quad i, j = 1, \cdots, n-1, |i-j| > 1; \end{aligned} \tag{133}$$

where $i \pm 1$ is a positive integer between 1 and $n-1$, and λ is called the loop parameter, a non-vanishing complex number. In this section, we study the Temperley–Lieb algebra $TL_n(\lambda)$ with the following type of idempotents:

$$e_i = \mathbb{1}^{\otimes(i-1)} \otimes T \otimes \mathbb{1}^{\otimes(n-i-1)}, \quad i = 1, 2, \cdots, n-1, \tag{134}$$

where $\mathbb{1}$ is the identity operator on the Hilbert space V and the generator T is a linear mapping on $V \otimes V$ to be specified in a given circumstance.

There is a well known diagrammatical representation to catch the essential algebraic properties of the Temperley–Lieb algebra $TL_n(\lambda)$, see [15]. In Figure 10, the generator e_i is depicted as a pair of cup and cap on the sites of i and $i+1$. The algebraic relations (133) defining the Temperley–Lieb algebra are read from the right to the left, while the corresponding diagrammatical expressions are read from the bottom to the top. The points on the same site (or in the same vertical row) are connected; the lines connecting points on different sites can be straightened via topological diagrammatical deformations, and two pairs of vanishing cups and caps contribute the normalization factor λ^{-2}.

A.2 The extended Temperley–Lieb diagrammatical representation for the Temperley–Lieb algebra generated by Bell states (5)

The fact that the EPR state (3), a maximal bipartite entangled state, generates a representation of the Temperley–Lieb algebra $TL_n(\lambda)$, has been discussed in [18], and here we make a brief sketch. The projector of the EPR state $|\Psi\rangle$ has the form

$$|\Psi\rangle\langle\Psi| = \frac{1}{d}\sum_{i,j=0}^{d-1} |ii\rangle\langle jj|, \tag{135}$$

with $d = 2$, the dimension of the Hilbert space V. With the T generator (134) given by $T = |\Psi\rangle\langle\Psi|$, the idempotents e_i of the Temperley–Lieb algebra $TL_n(\lambda)$ are defined as

$$e_i = \mathbb{1}_2^{\otimes(i-1)} \otimes |\Psi\rangle\langle\Psi| \otimes \mathbb{1}_2^{\otimes(n-i-1)}, \quad i = 1, 2, \cdots, n-1 \tag{136}$$

which naturally give rise to $e_i^2 = e_i$ and $e_i e_j = e_j e_i, \quad |i-j| > 1$. We calculate

$$e_1e_2e_1|\alpha\beta\gamma\rangle = \frac{1}{d}\sum_{l=0}^{d-1} e_1e_2|ll\gamma\rangle\delta_{\alpha\beta} = \frac{1}{d^3}\sum_{l=0}^{d-1}|nn\gamma\rangle\delta_{\alpha\beta} = \frac{1}{d^2}e_1|\alpha\beta\gamma\rangle, \tag{137}$$

to determine the loop parameter $\lambda = d = 2$.

Similarly, a representation of the Temperley–Lieb algebra $TL_n(\lambda)$ can be generated by the Bell states $|\psi(ij)\rangle$ (5), and the loop parameter is still $\lambda = d = 2$, see Subsubsection A.5.1. When the EPR state $|\Psi\rangle$ is described by the cup configuration and single-qubit gates are by solid points on the cup, the diagrammatical representation for the Temperley–Lieb algebra $TL_n(\lambda)$ generated by $|\psi(ij)\rangle\langle\psi(ij)|$ is the extended Temperley–Lieb diagrammatical configuration in [18].

The key reason that we propose such the extended Temperley–Lieb configuration is that it is capable of describing both quantum teleportation and teleportation-based quantum computation [9, 10, 11, 12, 13]. Such the diagrammatical representation is beyond the standard Temperley–Lieb diagrammatical representation in Figure 10, because the action of single-qubit and two-qubit quantum gates are not allowed by the defining algebraic relations of the Temperley–Lieb algebra (133) in general.

A.3 The Yang–Baxter equation and the Yang–Baxter gate

The Yang–Baxter equation [16] has the form

$$(R\otimes\mathbb{1})(\mathbb{1}\otimes R)(R\otimes\mathbb{1}) = (\mathbb{1}\otimes R)(R\otimes\mathbb{1})(\mathbb{1}\otimes R) \tag{138}$$

where R is a linear operator on $V\otimes V$. Note that it is also called the constant Yang–Baxter equation in the literature [16], because it has no explicit dependence on parameters.

It is well known that a solution of the Yang–Baxter equation (138) naturally yields a representation of the braid group $\mathcal{B}_n$ in low dimensional topology [15]. The braid group $\mathcal{B}_n$ has generators

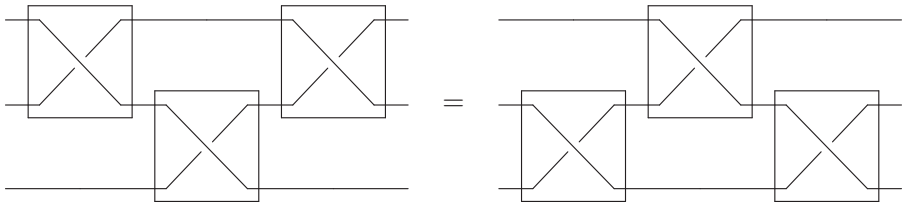

$$(R\otimes\mathbb{1})(\mathbb{1}\otimes R)(R\otimes\mathbb{1})=(\mathbb{1}\otimes R)(R\otimes\mathbb{1})(\mathbb{1}\otimes R)$$

Figure 11: Diagrammatical representation of the Yang–Baxter equation (138). Such the diagram without the boxes is the standard diagrammatical representation of the Yang–Baxter equation (138) in which a solution of the Yang–Baxter equation is denoted as an over-crossing braiding configuration. On the other hand, as the dimension of the Hilbert space V is $d = 2$, such the diagram is a quantum circuit model in terms of the Yang–Baxter gate which is a two-qubit gate represented by a box with two single-qubit lines.

$\sigma_1, \cdots, \sigma_{n-1}$, and the defining algebraic relations are

$$\begin{aligned}\sigma_i\sigma_{i+1}\sigma_i &= \sigma_{i+1}\sigma_i\sigma_{i+1}, \quad 1\leq i<n;\\ \sigma_i\sigma_j &= \sigma_j\sigma_i, \quad |i-j|>1.\end{aligned} \tag{139}$$

The braid group representation generated by a solution of the Yang–Baxter equation (138) usually takes the form

$$\sigma_i=\mathbb{1}^{\otimes(i-1)}\otimes R\otimes\mathbb{1}^{\otimes(n-i-1)}, \quad i=1,2,\cdots,n-1. \tag{140}$$

The Yang–Baxter gates [19, 20] are defined as unitary solutions of the Yang–Baxter equation [16] and satisfy the unitarity condition given by

$$R\,R^{\dagger}=R^{\dagger}R=\mathbb{1}. \tag{141}$$

In low dimensional topology [15], a solution of the Yang–Baxter equation is denoted as an over-crossing vertex. In quantum information and computation [1], a two-qubit quantum gate is represented as a box acting with two single-qubit lines. Hence, Figure 11 as the diagrammatical representation of the Yang–Baxter equation (with the two-dimensional identity operator) can be understood both in the viewpoint of low dimensional topology and in the viewpoint of quantum circuit model.

A.4 The Yang–Baxter gate via the Temperley–Lieb algebra

In this subsection, we present a detailed calculation on how to construct a type of the Yang–Baxter gates under the guidance of the state model construction of a type of solutions of the Yang–Baxter equation [15]. We find that the Yang–Baxter gate imposes the strict constraint condition on the loop parameter λ in the Temperley–Lieb algebra (133), whereas there is no such constraint on the loop parameter λ in the state model construction of a type of solutions of the Yang–Baxter equation [15].

In view of the state model in knot theory [15], we suppose that the Yang–Baxter gate R has the form,

$$R=a\mathbb{1}+bT, \tag{142}$$

where a and b are non-vanishing complex constants, and T is the type of generator in the construction (134) of the Temperley–Lieb algebra idempotents. Next, we specify the coefficients a

and b with the constraints of both the Yang–Baxter equation (138) and the unitary property (141) of quantum gates.

Substituting the Yang–Baxter gate (142) into the Yang–Baxter equation (138), after some algebra, we derive an equation of parameters a and b,

$$a^2 + ab + \frac{b^2}{\lambda^2} = 0. \tag{143}$$

Substituting the Yang–Baxter gate (142) into the unitarity condition (141), we have another constraint equations of parameters a and b,

$$\begin{cases} |a|^2 = 1; \\ a^*b + ab^* + |b|^2 = 0. \end{cases} \tag{144}$$

Now, let us take the complex conjugation of the equation (143) and then multiply the resultant equation with the equation (143), we obtain the equation

$$|a|^4 + |a|^2(a^*b + ab^* + |b|^2) = \frac{|b|^4}{|\lambda|^4}, \tag{145}$$

with the help of the unitarity constraint conditions (144), which can be simplified into the equation

$$|b|^2 = |\lambda|^2. \tag{146}$$

With the above constraint conditions on the coefficients a and b, we assume

$$a = e^{i\mu}, \quad b = |\lambda|e^{i\nu}, \tag{147}$$

with real parameters μ and ν, which give rise to the ratio of a and b,

$$\frac{a}{b} = \frac{1}{|\lambda|}e^{i(\mu-\nu)} = \frac{1}{|\lambda|}\cos(\mu-\nu) + \frac{i}{|\lambda|}\sin(\mu-\nu). \tag{148}$$

Thus it is much better directly to consider the equations of the parameter a/b. Reformulate the Yang–Baxter equation constraint condition (143) and the unitarity constraint condition (144) in terms of the parameter a/b respectively, and we have

$$\left(\frac{a}{b} + \frac{1}{2}\right)^2 = \frac{1}{4} - \frac{1}{\lambda^2}, \tag{149}$$

and

$$\frac{a}{b} + \frac{a^*}{b^*} = -1. \tag{150}$$

Clearly, there exists a constraint on the loop parameter λ, because the above three equations (148), (149) and (150) have to be consistent with one another. Combine the equation (148) with the equation (150), we have

$$\frac{1}{|\lambda|}\cos(\mu-\nu) = -\frac{1}{2}, \tag{151}$$

which gives the constraint for λ, that is $0 < |\lambda| \leq 2$. Similarly, with the relations (149) and (151), we have

$$\frac{\sin^2(\mu-\nu)}{|\lambda|^2} = \frac{1}{\lambda^2} - \frac{1}{4}, \tag{152}$$

which determines the loop parameter λ as a real number, $\lambda \in \mathbb{R}$, because $\sin^2(\mu-\nu)$ is a real number. Therefore, we are allowed to choose $0 < \lambda \leq 2$ for convenience, since only λ^2 appears in the defining algebraic relations of the Temperley–Lieb algebra (133).

Obviously, the Yang–Baxter gate (142) modulo a phase factor is still a unitary solution of both the Yang–Baxter equation (138) and the unitarity constraint equation (141), thus we set the coefficient a as 1 and then multiply the Yang–Baxter gate with the globe phase factor $e^{i\mu}$. Finally, with the coefficients a and b given by

$$a = e^{i\mu}, \quad b = -\frac{\lambda}{2}(\lambda \pm i\sqrt{4-\lambda^2})e^{i\mu}, \tag{153}$$

we have the Yang–Baxter gate via the Temperley–Lieb algebra, expressed as

$$R = e^{i\mu}(\mathbb{1} - \frac{\lambda}{2}(\lambda \pm i\sqrt{4-\lambda^2})T). \tag{154}$$

To be clarified again, the range of the loop parameter λ, $0 < \lambda \leq 2$[6], is determined by both the Yang–Baxter equation (138) and the unitarity constraint equation (141), so it is independent of the dimension of the chosen Hilbert space V.

A.5 Examples for the Yang–Baxter gate via the Temperley–Lieb algebra

We present typical examples for the Yang–Baxter gate via the Temperley–Lieb algebra, and they are respectively about $\lambda = 2$ and $\lambda = \sqrt{2}$. They are to be exploited in this paper because the dimension of the associated Hilbert space is $d = 2$, the dimension of a qubit [1, 2].

A.5.1 Type I Yang–Baxter gate for $\lambda = 2$ and its extended Temperley–Lib diagrammatical representation

For the case of $\lambda = 2$, we solve the equations (153) and obtain the Yang–Baxter gate as

$$R_I(\pm 1, \tau) = \mathbb{1} - 2T_I(\pm 1, \tau) \tag{155}$$

modulo a global phase factor $e^{i\mu}$, with a parameter τ to be determined, which is called the type I Yang–Baxter gate in this paper. In the literature, see [35] (and its quoted earlier references), a suitable representation for T_I in the two-qubit Hilbert space, has the form

$$T_I(1,\tau) = \frac{1}{2}\begin{pmatrix} 1 & 0 & 0 & \tau \\ 0 & 0 & 0 & 0 \\ 0 & 0 & 0 & 0 \\ \tau^{-1} & 0 & 0 & 1 \end{pmatrix} \quad \text{or} \quad T_I(-1,\tau) = \frac{1}{2}\begin{pmatrix} 0 & 0 & 0 & 0 \\ 0 & 1 & \tau & 0 \\ 0 & \tau^{-1} & 1 & 0 \\ 0 & 0 & 0 & 0 \end{pmatrix}, \tag{156}$$

where τ is a complex number with norm 1, so the type I Yang–Baxter gate R has the form

$$R_I(1,\tau) = \begin{pmatrix} 0 & 0 & 0 & -\tau \\ 0 & 1 & 0 & 0 \\ 0 & 0 & 1 & 0 \\ -\tau^{-1} & 0 & 0 & 0 \end{pmatrix} \quad \text{or} \quad R_I(-1,\tau) = \begin{pmatrix} 1 & 0 & 0 & 0 \\ 0 & 0 & -\tau & 0 \\ 0 & -\tau^{-1} & 0 & 0 \\ 0 & 0 & 0 & 1 \end{pmatrix}. \tag{157}$$

The T_I matrix (156) can be respectively written as a projector generated by the EPR state (3) with the local action of the single-qubit gate,

$$T_I(1,\tau) = (\mathbb{1}_2 \otimes L)|\psi(00)\rangle\langle\psi(00)|(\mathbb{1}_2 \otimes L^\dagger) \tag{158}$$

$$T_I(-1,\tau) = (\mathbb{1}_2 \otimes XL)|\psi(00)\rangle\langle\psi(00)|(\mathbb{1}_2 \otimes L^\dagger X), \tag{159}$$

with the single-qubit gate L given by

$$L = \begin{pmatrix} 1 & 0 \\ 0 & \tau^{-1} \end{pmatrix} \tag{160}$$

[6]The case for the loop parameter $\lambda = 2$ has been discussed in [19].

where $L = \mathbb{1}_2$ for $\tau = 1$ and $L = Z$ for $\tau = -1$. So the type I Yang–Baxter gate $R_I(1,\tau)$ (157) has the extended Temperley–Lieb diagrammatical representation,

$R_I(1,\tau) =$ 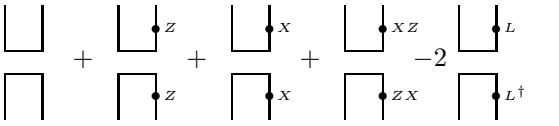

, (161)

and the type I Yang–Baxter gate $R_I(-1,\tau)$ (157) has the other extended Temperley–Lieb diagrammatical representation,

$R_I(-1,\tau) =$ 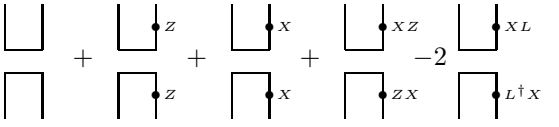

. (162)

In this paper, we only consider the special type I Yang–Baxter gates for the cases $\tau = \pm 1$, which are denoted by the Yang–Baxter gates $R(ij)$ (71),

$$\begin{aligned} &R(00) = R_I(1,1), \quad R(01) = R_I(1,-1), \\ &R(10) = R_I(-1,1), \quad R(11) = R_I(-1,-1), \end{aligned} \tag{163}$$

and the associated T_I matrices (156) are respectively related to four projectors of the Bell states $|\psi(ij)\rangle$ (5),

$$\begin{aligned} &|\psi(00)\rangle\langle\psi(00)| = T_I(1,1), \quad |\psi(01)\rangle\langle\psi(01)| = T_I(1,-1), \\ &|\psi(10)\rangle\langle\psi(10)| = T_I(-1,1), \quad |\psi(11)\rangle\langle\psi(11)| = T_I(-1,-1), \end{aligned} \tag{164}$$

which have been used in Subsection A.2. The extended Temperley–Lieb diagrammatical representation for the Yang–Baxter gate $R(ij)$ is presented in Subsection 4.2.

A.5.2 Type II Yang–Baxter gate for $\lambda = \sqrt{2}$ and its extended Temperley–Lieb diagrammatical representation

For the case of $\lambda = \sqrt{2}$, we solve the equations (153) and have the solutions,

$$a = e^{i\mu}, \quad b = -\sqrt{2} e^{\pm i\frac{\pi}{4}} e^{i\mu} \tag{165}$$

and with the suitable phase factors $e^{i\mu}$, we have two kinds of the type II Yang–Baxter gates,

$$R_{II}(+) = e^{i\frac{\pi}{4}} \mathbb{1} - i\sqrt{2} T_{II}, \quad R_{II}(-) = e^{-i\frac{\pi}{4}} \mathbb{1} + i\sqrt{2} T_{II}, \tag{166}$$

where $\mu = \pi/4$ in $R_{II}(+)$ and $\mu = -\pi/4$ in $R_{II}(-)$.

We exploit the representation of T_{II} in the two-qubit Hilbert space, which is shown in [35] (and its quoted earlier references),

$$T_{II}(\epsilon,\varphi) = \frac{1}{2} \begin{pmatrix} 1 & 0 & 0 & -ie^{-i\varphi} \\ 0 & 1 & -i\epsilon & 0 \\ 0 & i\epsilon & 1 & 0 \\ ie^{i\varphi} & 0 & 0 & 1 \end{pmatrix}, \tag{167}$$

and the associated Yang–Baxter gates $R_{II}(+)$ and $R_{II}(-)$ can have a unified formalism,

$$\begin{aligned} R(\epsilon,\varphi) &= e^{-i\frac{\pi}{4}}\mathbb{1}_4 + i\sqrt{2}T_{II} \\ &= \frac{1}{\sqrt{2}}\begin{pmatrix} 1 & 0 & 0 & e^{-i\varphi} \\ 0 & 1 & \epsilon & 0 \\ 0 & -\epsilon & 1 & 0 \\ -e^{i\varphi} & 0 & 0 & 1 \end{pmatrix}, \end{aligned} \tag{168}$$

with $\epsilon = \pm 1$. About the application of the type II Yang–Baxter gate $R(\epsilon,\varphi)$ to quantum information and computation, interested readers are invited to refer to [21].

The $T_{II}(\epsilon,\varphi)$ matrix (167) can be formulated as a sum of two projectors, each of which is generated by the Bell states with the local action of single-qubit gates,

$$T_{II}(\epsilon,\varphi) = |\psi_\varphi(00)\rangle\langle\psi_\varphi(00)| + |\psi_\epsilon(10)\rangle\langle\psi_\epsilon(10)|, \tag{169}$$

where $|\psi_\varphi(00)\rangle$ and $|\psi_\epsilon(10)\rangle$ are respectively given by

$$\begin{aligned} |\psi_\varphi(00)\rangle &= \frac{1}{\sqrt{2}}(\mathbb{1}_2 \otimes M)|\psi(00)\rangle, \\ |\psi_\epsilon(10)\rangle &= \frac{1}{\sqrt{2}}(\mathbb{1}_2 \otimes XN)|\psi(00)\rangle, \end{aligned} \tag{170}$$

with the single-qubit gates M and N given by

$$M = \begin{pmatrix} 1 & 0 \\ 0 & ie^{i\varphi} \end{pmatrix}, \quad N = \begin{pmatrix} 1 & 0 \\ 0 & i\epsilon \end{pmatrix}. \tag{171}$$

Consequently, the type II Yang–Baxter gate $R(\epsilon,\varphi)$ (168) has the extended Temperley–Lieb configuration,

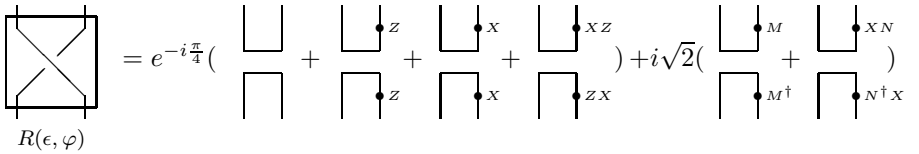

(172)

where the extended Temperley–Lieb configuration (69) of the two-qubit identity gate is exploited.

In this paper, we consider the special type II Yang–Baxter gates, denoted by the $B(\epsilon,\eta)$ gate (75), satisfying

$$B(\epsilon,1) = R(\epsilon,0), \quad B(\epsilon,-1) = R(\epsilon,\pi), \tag{173}$$

which are the Bell transform introduced in [13], and apply them to the study of teleportation-based quantum computation in Section 5.

Note that the same quantum gate allows various of the extended Temperley–Lieb diagrammatical representations, and the reason is that single-qubit gates acting on such the configuration can be chosen in purpose. For example, the extended Temperley–Lieb configuration (80) for the special type II Yang–Baxter gate $B(\epsilon,\eta)$ (75) is essentially equivalent to that one obtained from the extended Temperley–Lieb configuration (172) of the type II Yang–Baxter gate $R(\epsilon,\varphi)$ (168) by taking φ as 0 or π, but they indeed look different in form.

A.5.3 Type III Yang–Baxter gate: $\lambda = \sqrt{3}$

For the case of $\lambda = \sqrt{3}$, we solve the equations (153) and obtain the third type of the Yang–Baxter gate as

$$R_{III} = \mathbb{1} - \sqrt{3}\, e^{\pm i\frac{\pi}{6}}\, T_{III} \tag{174}$$

modulo a global phase factor $e^{i\mu}$. In the literature [35], two kinds of the T_{III} matrices have been constructed with the associate dimension of the Hilbert space, $d = 3$, which are not directly related to the main topic of this paper so are not presented here.

A.6 Remarks on further research

With our research results in this paper, we suggest two interesting configurations for both physicists in quantum information and computation [1] and mathematicians in low dimensional topology [15]: the one is the extended Temperley–Lieb diagrammatical configuration, and the other is the extended braiding configuration (the braiding gate is the Yang–Baxter gate) with the action of quantum gates. Here we propose five open problems for interested readers as follows.

The first problem is how to construct more nontrivial examples for the Yang–Baxter gates via the Temperley–Lieb algebra, besides the above three types of examples: $\lambda = 2$ in Subsubsection A.5.1, $\lambda = \sqrt{2}$ in Subsubsection A.5.2 and $\lambda = \sqrt{3}$ in Subsubsection A.5.3. The papers in [35] and its quoted earlier references may be helpful for solving this problem in a systematic approach. Note that $0 < \lambda \leq 2$ is derived in the present paper.

The second problem is to study the algebraic formulation of the extended Temperley–Lieb algebraic approach. The reason for it is that the diagrammatical representation of both quantum teleportation and teleportation-based quantum computation is the extended Temperley–Lieb configuration. Obviously, the Temperley–Lieb algebra (133) is to be a special example of such the algebraic structure, if it exists. Interested readers are invited to refer to [18, 36] for some insights on this problem.

The third problem is how to construct solutions of the Yang–Baxter equation directly in the extended Temperley–Lieb diagrammatical approach. Note that all of our examples for the Yang–Baxter gates in this paper are constructed using the Temperley–Lieb algebra, although they admit the extended Temperley–Lieb representations. So it is meaningful to study solutions of the Yang–Baxter equation which are not associated with the Tempereley–Lieb algebra but have the extended Temperley–Lieb diagrammatical representation. For example, we can construct the Yang–Baxter gates using the Birman-Wenzl-Murakami algebra [37] instead of the Temperley–Lieb algebra.

The fourth problem is to study the algebraic structure underlying the braiding configuration with the local actions of single-qubit gates. It is an interesting question, because our results clearly show that this kind of configuration is capable of describing teleportation-based quantum computation. If such the algebraic structure exists, it will be directly related to the algebraic formulation of the extended Temperley–Lieb configuration.

The fifth problem is to study a possibility of constructing a new type of the state model [15] (or a new type of knot invariants) using the extended Temperley–Lieb diagrammatical configuration of the braiding gate (the Yang–Baxter gate). Such the research may bring a new way of thinking about the relationship between topological entanglement and quantum entanglement [22].

As a conclusion of this section, we want to emphasize the last thing that quantum information and computation indeed offers both mathematicians and mathematical physicists a lot of interesting problems to solve. For example, the above problems are just motivated by our study on both topological and algebraic descriptions of teleportation-based quantum computation.

B The special type I Yang–Baxter gates (71) are permutation-like quantum gates

In this paper, we do not apply the special type I Yang–Baxter gates (71) to teleportation-based quantum computation, and for readers' convenience, a brief study on the algebraic properties of the special type I Yang–Baxter gates (71) is performed in the following.

The special type I Yang–Baxter gate $R(ij)$ (71) has the matrix form

$$R(ij) = \sum_{k,l=0}^{1} (1-2\delta_{i,k}\delta_{j,l})|\psi(kl)\rangle\langle\psi(kl)| \tag{175}$$

$$= \begin{pmatrix} 1-\delta_{i,0} & 0 & 0 & (-1)^{j+1}\delta_{i,0} \\ 0 & 1-\delta_{i,1} & (-1)^{j+1}\delta_{i,1} & 0 \\ 0 & (-1)^{j+1}\delta_{i,1} & 1-\delta_{i,1} & 0 \\ (-1)^{j+1}\delta_{i,0} & 0 & 0 & 1-\delta_{i,0} \end{pmatrix}, \tag{176}$$

where the symbol δ denotes the Kronecker delta function, so each $R(ij)$ gate has four non-vanishing matrix entries, for example, the Yang–Baxter gate $R(11)$ is the Permutation gate P (72).

With the relation (5) that the four Bell states are transformed to one another by local Pauli gates, the special type I Yang–Baxter gates $R(ij)$ can be rewritten as the Permutation gate P (72) with the local action of Pauli gates,

$$R(ij) = Z_1^{j+1}X_1^{i+1}PX_1^{i+1}Z_1^{j+1} = X_2^{i+1}Z_2^{j+1}PZ_2^{j+1}X_2^{i+1}, \tag{177}$$

where the subscripts 1 and 2 denote the qubit sites that the associated Pauli gates are acting on. Since the entangling power [26] of both the Permutation gate P and local single-qubit gates is zero, then the entangling power of the special type I Yang–Baxter gates $R(ij)$ is zero. In other words, the two-qubit quantum gates $R(ij)$ with the action of arbitrary single-qubit gates can not perform universal quantum computation [1], which is the key reason that we do not apply the special type I Yang–Baxter gate to teleportation-based quantum computation in this paper.

In terms of the special type I Yang–Baxter gate, we define the teleportation swapping operator [18], denoted by $S(ij)$,

$$\begin{aligned} S(ij) &= R(ij)_{23}R(ij)_{12}R(ij)_{23} = R(ij)_{12}R(ij)_{23}R(ij)_{12} \\ &= Z_2^{j+1}X_2^{i+1}P_{23}P_{12}P_{23}X_2^{i+1}Z_2^{j+1}, \end{aligned} \tag{178}$$

where $R(ij)_{23} = \mathbb{1}_2 \otimes R(ij)$ and $R(ij)_{12} = R(ij) \otimes \mathbb{1}_2$. The teleportation swapping operator $S(ij)$ acting on the product state of arbitrary three qubit states $|\lambda\rangle \otimes |\mu\rangle \otimes |\nu\rangle$, gives rise to the result

$$S(ij)(|\lambda\rangle \otimes |\mu\rangle \otimes |\nu\rangle) = |\nu\rangle \otimes |\mu\rangle \otimes |\lambda\rangle, \tag{179}$$

where the first qubit $|\lambda\rangle$ and the third qubit $|\nu\rangle$ have been swapped with each other.

C Topological construction of the four-qubit state $|\Psi_{CNOT}^{\uparrow}\rangle$

Compared with the four-qubit entangled state $|\Psi_{CNOT}\rangle$ (29), the other four-qubit entangled state $|\Psi_{CNOT}^{\uparrow}\rangle$ takes the form

$$|\Psi_{CNOT}^{\uparrow}\rangle_{1256} = (\mathbb{1}_2 \otimes CNOT_{52} \otimes \mathbb{1}_2)|\Psi\rangle_{12} \otimes |\Psi\rangle_{56}, \tag{180}$$

with the extended Temperley–Lieb diagrammatical representation

$|\Psi_{CNOT}^{\uparrow}\rangle =$ 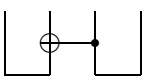 (181)

in which the $CNOT_{52}$ gate has the fifth qubit as the control qubit and the second qubit as the target qubit.

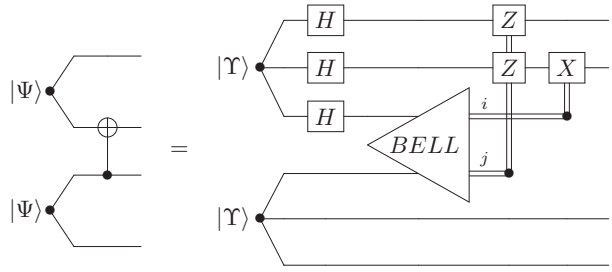

Figure 12: Quantum circuit for the construction of the four-qubit entangled state $|\Psi^{\uparrow}_{CNOT}\rangle$ (180), as the diagrammatical representation of the teleportation equation (182). After performing the Bell measurements on the third and fourth qubits of the six-qubit state $H_1H_2H_3|\Upsilon\rangle_{123}|\Upsilon\rangle_{456}$, according to the measurement results, we perform the local unitary correction gate $X_2^iZ_1^jZ_2^j$ to complete the construction.

In order to construct the $|\Psi^{\uparrow}_{CNOT}\rangle$ state, we prepare the six-qubit state $H_1H_2H_3|\Upsilon\rangle_{123}|\Upsilon\rangle_{456}$ and perform the Bell measurements on its third and fourth qubits, and such the procedure gives rise to the teleportation equation

$$H_1H_2H_3|\Upsilon\rangle_{123}|\Upsilon\rangle_{456} = \sum_{i,j=0}^{1} |\psi(ij)\rangle Z_1^jZ_2^jX_2^i|\Psi^{\uparrow}_{CNOT}\rangle_{1256}, \tag{182}$$

which is associated with the quantum circuit model in Figure 12.

In the extended Temperley–Lieb diagrammatical approach, using the diagrammatical representation (54) of the $H_1H_2H_3|\Upsilon\rangle_{123}$ state and the diagrammatical representation (51) of the $|\Upsilon\rangle_{456}$ state and the diagrammatical representation (38) of the Bell measurement, we have the topological diagrammatical representation of the teleportation equation (182),

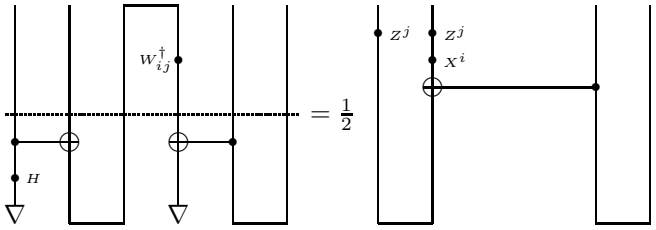

(183)

in which we move the single-qubit gate $W_{ij}^{\dagger}$ from the fourth qubit to the second qubit and across the $CNOT_{12}$ gate via the formula

$$CNOT_{12}(\mathbb{1}_2 \otimes W_{ij}^{\dagger})CNOT_{12} = Z_1^jZ_2^jX_2^i; \tag{184}$$

then interchange the $CNOT_{12}$ gate and the $CNOT_{52}$ gate, and finally apply the diagrammatical representation (47) of the EPR state $|\Psi\rangle$.

Furthermore, on the diagram (183), we replace the configuration of the $H_1H_2H_3|\Upsilon\rangle_{123}$ state with its another equivalent configuration (56) and replace the configuration of the $|\Upsilon\rangle_{456}$ state

with its another equivalent configuration (53) to obtain the other diagram,

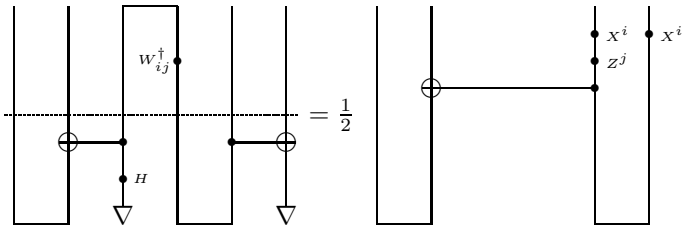

(185)

in which moving the single-qubit gate $W_{ij}^{\dagger}$ across the $CNOT_{56}$ gate involves the formula

$$CNOT_{56}(W_{ij} \otimes \mathbb{1}_2)CNOT_{56} = X_5^i X_6^i Z_5^j. \tag{186}$$

With the topological diagrammatical representation (185), we derive its algebraic counterpart as

$$H_1 H_2 H_3 \, |\Upsilon\rangle_{123} |\Upsilon\rangle_{456} = \sum_{i,j=0}^{1} |\psi(ij)\rangle X_5^i X_6^i Z_5^j |\Psi_{CNOT}^{\uparrow}\rangle_{1256}, \tag{187}$$

which is equivalent to the teleportation equation (182).

D Topological construction of the four-qubit state $|\Psi_{CZ}\rangle$

The four-qubit entangled state $|\Psi_{CZ}\rangle$ used to perform CZ gate (13) in teleportation-based quantum computation, takes the form

$$|\Psi_{CZ}\rangle_{1256} = (\mathbb{1}_2 \otimes CZ_{25} \otimes \mathbb{1}_2)(|\Psi\rangle_{12} \otimes |\Psi\rangle_{56}), \tag{188}$$

with the extended Temperley–Lieb diagrammatical form

$$|\Psi_{CZ}\rangle = \tag{189}$$

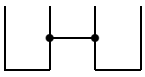

in which two solid points linked by the horizontal line represents the CZ gate and the symmetrical diagrammatical notation of the CZ gate indicates $CZ_{25} = CZ_{52}$.

With the algebraic relation between the $|\Psi_{CZ}\rangle$ state and the other four-qubit entangled state $|\Psi_{CNOT}\rangle$ (29) given by

$$|\Psi_{CZ}\rangle_{1256} = H_5 \, H_6 \, |\Psi_{CNOT}\rangle_{1256}, \tag{190}$$

we obtain the teleportation equation for the construction of the $|\Psi_{CZ}\rangle$ state directly from the teleportation equation (30) for the construction of the $|\Psi_{CNOT}\rangle$ state,

$$H_4 |\Upsilon\rangle_{123} |\Upsilon\rangle_{456} = \sum_{i,j=0}^{1} |\psi(ij)\rangle_{34} \; Z_2^j X_1^i X_2^i |\Psi_{CZ}\rangle_{1256}, \tag{191}$$

which has the associated quantum circuit model in Figure 13.

Using the diagrammatical representation (51) of the three-qubit GHZ state $|\Upsilon\rangle$ and the diagrammatical representation (38) of the Bell measurement, we have the topological diagrammatical representation of the teleportation equation (191),

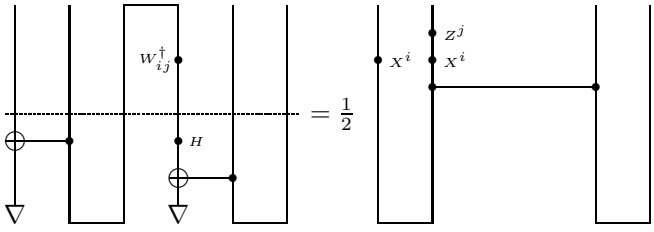

(192)

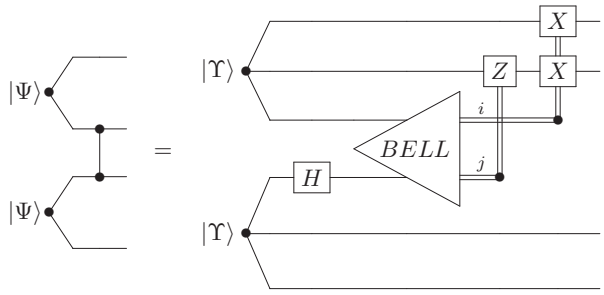

Figure 13: Quantum circuit for the construction of the four-qubit entangled state $|\Psi_{CZ}\rangle$ (188) as the diagrammatical representation of the teleportation equation (191).

in which we firstly move the single-qubit gate $W_{ij}^{\dagger}$ gate from the fourth qubit to the second qubit and across the $CNOT_{21}$ gate via the formula

$$CNOT_{21}(\mathbb{1}_2 \otimes W_{ij}^{\dagger})CNOT_{21} = Z_2^j X_1^i X_2^i; \tag{193}$$

secondly perform the topological straightening operation to derive the normalization factor $\frac{1}{2}$ after moving the Hadamard gate from the fourth qubit to the second qubit; thirdly apply the relation $H_2 CNOT_{52} H_2 = CZ_{25}$ between the $CNOT$ gate and the CZ gate and then interchange the $CNOT_{21}$ gate with the CZ_{25} gate; and finally use the diagrammatical representation (49) of the EPR state $|\Psi\rangle$.

On the other hand, with the diagrammatical representation (53) of the three-qubit GHZ state $|\Upsilon\rangle$, the diagram (192) has the other equivalent representation

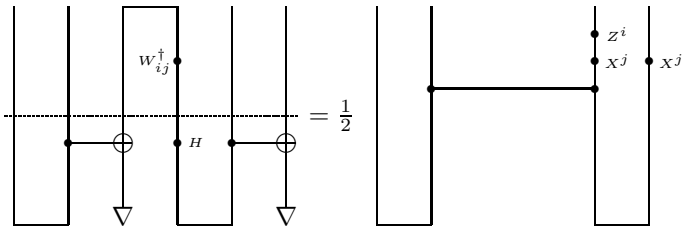

(194)

in which the single-qubit gate $W_{ij}^{\dagger} H$ gate is moved from the fourth qubit to the fifth qubit and across the $CNOT_{56}$ gate via the formula

$$CNOT_{56}(H \otimes \mathbb{1}_2)(W_{ij} \otimes \mathbb{1}_2)(H \otimes \mathbb{1}_2)CNOT_{56} = Z_5^i X_5^j X_6^j, \tag{195}$$

then the algebraic relation $H_5 CNOT_{25} H_5 = CZ_{25}$ is used to derive the CZ_{25} gate, and the CZ_{25} gate and the $CNOT_{56}$ gate are interchanged to apply the diagrammatical representation (47) of the EPR state $|\Psi\rangle$. Such the topological diagrammatical representation (194) admits the form of the teleportation equation

$$H_4|\Upsilon\rangle_{123}|\Upsilon\rangle_{456} = \sum_{i,j=0}^{1} |\psi(ij)\rangle_{34}\ Z_5^i X_5^j X_6^j |\Psi_{CZ}\rangle_{1256}, \tag{196}$$

which is obviously the other equivalent form of the teleportation equation (191).

E An algebraic method of deriving both the extended Temperley–Lieb configuration in Figure 9 and the algebraic expansion (131) of the teleportation operator $(B \otimes \mathbb{1}_2)(\mathbb{1}_2 \otimes B)$

Let us make an algebraic study of how to derive the extended Temperley–Lieb configuration in Figure 9, which is originally derived in the diagrammatical approach. First of all, we introduce the algebraic notation for the typical extended Temperley–Lieb configurations in teleportation-based quantum computation,

$$\begin{aligned}((U_1, U_2), \mathbb{1}_2) &\equiv |\Psi_{U_1}\rangle\langle\Psi_{U_2}| \otimes \mathbb{1}_2 \\ (\mathbb{1}_2, (U_3, U_4)) &\equiv \mathbb{1}_2 \otimes |\Psi_{U_3}\rangle\langle\Psi_{U_4}| \\ (U_1, U_3U_2^T, U_4) &\equiv (|\Psi_{U_1}\rangle\langle\Psi| \otimes U_3U_2^T)(\mathbb{1}_2 \otimes |\Psi\rangle\langle\Psi_{U_4}|)\end{aligned} \tag{197}$$

with $|\Psi_U\rangle$ defined in (19), and we have the formula as

$$((U_1, U_2), \mathbb{1}_2)(\mathbb{1}_2, (U_3, U_4)) = (U_1, U_3U_2^T, U_4) \tag{198}$$

to characterize the diagrammatical representation,

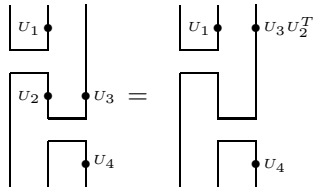

in which U_2^T is obtained by moving U_2 from the second qubit to the third qubit. Applying the formula (198), the teleportation operator $(B \otimes \mathbb{1}_2)(\mathbb{1}_2 \otimes B)$ can be reformulated as

$$\begin{aligned}&(B \otimes \mathbb{1}_2)(\mathbb{1}_2 \otimes B) \\ =&(Z, \mathbb{1}_2, \mathbb{1}_2) + (Z, Z, \mathbb{1}_2) + (X, X, \mathbb{1}_2) - (X, XZ, \mathbb{1}_2) \\ &-(\mathbb{1}_2, \mathbb{1}_2, Z) + (\mathbb{1}_2, Z, Z) - (XZ, X, Z) - (XZ, XZ, Z) \\ &+(Z, X, X) + (Z, XZ, X) + (X, \mathbb{1}_2, X) - (X, Z, X) \\ &-(\mathbb{1}_2, X, ZX) + (\mathbb{1}_2, XZ, ZX) - (XZ, \mathbb{1}_2, ZX) - (XZ, Z, ZX),\end{aligned} \tag{199}$$

each term of which corresponds to the relevant diagrammatical term in Figure 9.

With the result (199), furthermore, we are able to derive the algebraic expansion (131) of the teleportation operator $(B \otimes \mathbb{1}_2)(\mathbb{1}_2 \otimes B)$. Before calculation, we introduce the notation

$$(|ij\rangle, W_{1,1}, \langle kl|) \equiv (|ij\rangle\langle\Psi| \otimes W_{1,1})(\mathbb{1}_2 \otimes |\Psi\rangle\langle kl|), \tag{200}$$

which has already appeared in (131), and with it, for example, we verify the formula

$$(Z, \mathbb{1}_2, \mathbb{1}_2) - (\mathbb{1}_2, \mathbb{1}_2, Z) = (|00\rangle, \mathbb{1}_2, \langle 11|) - (|11\rangle, \mathbb{1}_2, \langle 00|), \tag{201}$$

characterized by the topological configuration

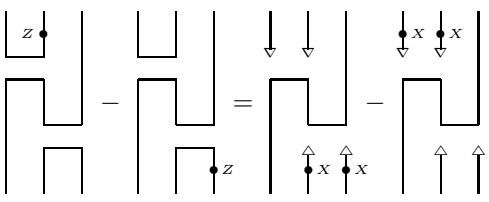

(202)

where the vertical line with ∇ stands for the $|0\rangle$ state. With the technique underlying the formula (201), we rewrite the algebraic expression (199) into

$$\begin{aligned}
&(B\otimes \mathbb{1}_2)(\mathbb{1}_2\otimes B)\\
=&(|00\rangle, Z, \langle 00|) - (|01\rangle, XZ, \langle 00|) + (|10\rangle, X, \langle 00|) - (|11\rangle, \mathbb{1}_2, \langle 00|)\\
+&(|00\rangle, XZ, \langle 01|) - (|01\rangle, Z, \langle 01|) + (|10\rangle, \mathbb{1}_2, \langle 01|) - (|11\rangle, X, \langle 01|)\\
+&(|00\rangle, X, \langle 10|) + (|01\rangle, \mathbb{1}_2, \langle 10|) - (|10\rangle, Z, \langle 10|) - (|11\rangle, XZ, \langle 10|)\\
+&(|00\rangle, \mathbb{1}_2, \langle 11|) + (|01\rangle, X, \langle 11|) - (|10\rangle, XZ, \langle 11|) - (|11\rangle, Z, \langle 11|)
\end{aligned} \tag{203}$$

which is the algebraic expanded formalism (131) of the teleportation operator $(B\otimes \mathbb{1}_2)(\mathbb{1}_2\otimes B)$.

References

[1] M.A.Nielsen and I.L. Chuang, *Quantum Computation and Quantum Information*, (Cambridge University Press, Cambridge, UK, 2000 and 2011).

[2] J. Preskill, *Lecture Notes on Quantum Computation*, http://www.theory.caltech.edu/preskill.

[3] A. Einstein, B. Podolsky, and N. Rosen, *Can Quantum-Mechanical Description of Physical Reality be Considered Complete?*, Phys. Rev. **47**, 777-780 (1935).

[4] J.S. Bell, *On the Einstein-Podolsky-Rosen paradox*, Physics **1** 195-200 (1964).

[5] C.H. Bennett, G. Brassard, C. Crepeau, R. Jozsa, A. Peres and W.K. Wootters, *Teleporting an Unknown Quantum State via Dual Classical and Einstein-Podolsky-Rosen Channels*, Phys. Rev. Lett. **70** 1895 (1993).

[6] L. Vaidman, *Teleportation of Quantum States*, Phys. Rev. A **49**, 1473-1475 (1994).

[7] S.L. Braunstein, G.M. D'Ariano, G.J. Milburn and M.F. Sacchi, *Universal Teleportation with a Twist*, Phys. Rev. Let. **84**, 3486-3489 (2000).

[8] R. F. Werner, *All Teleportation and Dense Coding Schemes*, J.Phys. A: Math. Theor. **35**, 7081-7094 (2001).

[9] D. Gottesman and I. Chuang, *Demonstrating the Viability of Universal Quantum Computation Using Teleportation and Single-Qubit Operations*, Nature **402**, 390 (1999).

[10] M.A. Nielsen, *Universal Quantum Computation Using Only Projective Measurement, Quantum Memory, and Preparation of the* 0 *State*, Phys. Lett. A **308**, 96 (2003).

[11] D.W. Leung, *Quantum Computation by Measurements*, Int. J. Quantum Inf. **2**, 33 (2004).

[12] Y. Zhang and J-L. Pang, *Space-Time Topology in Teleportation-Based Quantum Computation*, arXiv:1309.0955 (2013).

[13] Y. Zhang and K. Zhang, *Bell Transform, Teleportation Operator and Teleportation-Based Quantum Computation*, arXiv:1401.7009 (2014).

[14] H.N.V. Temperley and E.H. Lieb, *Relations between the 'Percolation' and 'Colouring' Problem and Other Graph-Theoretical Problems Associated with Regular Planar Lattices: Some Exact Results for the 'Percolation' Problem*, Proc. Roy. Soc. A **322**, 251(1971).

[15] L. H. Kauffman, *Knots and Physics* (World Scientific Publishers, 2002).

[16] C.N. Yang, *Some Exact Results for the Many Body Problems in One Dimension with Repulsive Delta Function Interaction*, Phys. Rev. Lett. **19**, 1312-1314 (1967). R.J. Baxter, *Partition Function of the Eight-Vertex Lattice Model*, Annals Phys. **70**, 193-228 (1972). J.H.H. Perk and H. Au-Yang, *Yang–Baxter Equations*, Encyclopedia of Mathematical Physics, Vol. 5, 465-473 (Elsevier Science, Oxford, 2006).

[17] L.H. Kauffman, *Teleportation Topology*. Opt. Spectrosc. **9**, 227 (2005).

[18] Y. Zhang, *Teleportation, Braid Group and Temperley–Lieb Algebra*, J.Phys. A: Math. Theor. **39**, 11599-11622 (2006); Y. Zhang and L.H. Kauffman, *Topological-Like Features in Diagrammatical Quantum Circuits*, Quant. Inf. Proc. **6**, 477-507 (2007); Y. Zhang, *Braid Group, Temperley–Lieb Algebra, and Quantum Information and Computation*, AMS Contemporary Mathematics **482**, 52 (2009).

[19] H. Dye, *Unitary Solutions to the Yang–Baxter Equation in Dimension Four*, Quantum Inform. Process. **2**, 117-150 (2003).

[20] L.H. Kauffman and S.J. Lomonaco Jr., *Braiding Operators are Universal Quantum Gates*, New Journal of Physics **6**, 134 (2004).

[21] Y. Zhang, L.H. Kauffman and M.L. Ge, *Universal Quantum Gate, Yang–Baxterization and Hamiltonian*. Int. J. Quant. Inform. **4**, 669-678 (2005).

[22] L.H. Kauffman and S. J. Lomonaco Jr., *Quantum Entanglement and Topological Entanglement*, New Journal of Physics, **4**, 73 (2002).

[23] A. Barenco et al., *Elementary Gates for Quantum Computation*, Phys. Rev. A **52**, 3457-3467 (1995).

[24] J.L. Brylinski and R. Brylinski, *Universal Quantum Gates*, in *Mathematics of Quantum Computation*, Chapman & Hall/CRC Press, Boca Raton, Florida, 2002 (edited by R. Brylinski and G. Chen).

[25] P.O. Boykin, T. Mor, M. Pulver, V. Roychowdhury and F. Vatan, *A New Universal and Fault-Tolerant Quantum Basis*, Inf. Process. Lett, **75**, 101-107 (2000).

[26] D.J. Brod and E.F. Galvão, *Extending Matchgates into Universal Quantum Computation*, Phys. Rev. A, **84**, 022310 (2011).

[27] R. Raussendorf and H.J. Briegel, *A One-Way Quantum Computer*, Phys. Rev. Lett. **86**, 5188 (2001).

[28] D. Gottesman, *Stabilizer Codes and Quantum Error Correction Codes*, Ph.D. Thesis, CalTech, Pasadena, CA, 1997.

[29] D.M. Greenberger, M.A. Horne, A. Shirnony, and A.Zeilinger, *Bell's Theorem Without Inequalities*, Am. J. Phys. **58**, 1131 (1990).

[30] A.M. Childs, *Teleportation-based Approaches to Universal Quantum Computation with Single-Qubit Measurement*, Seminar at the Perimeter Institute, November 2003.

[31] P. Bonderson, M. Freedman and C. Nayak, *Measurement-Only Topological Quantum Computation*, Phys. Rev. Lett. **101**, 010501 (2008)

[32] B. Coecke, *The Logic of Entanglement. An Invitation*. Oxford University Computing Laboratory Research Report nr. PRG-RR-03-12. An 8 page short version is at Arxiv:quant-ph/0402014. The full 160 page version is at "web.comlab.ox.ac.uk/oucl/publications/tr/rr-03-12.html".

[33] S. Abramsky and B. Coecke, *A Categorical Semantics of Quantum Protocols*. In: Proceedings of the 19th Annual IEEE Symposium on Logic in Computer Science (LiCS'04), IEEE Computer Science Press.

[34] S. Abramsky, *Temperley–Lieb Algebra: from Knot Theory to Logica and Computation via Quantum Mechanics*, arXiv:0910.2737 (2009).

[35] K. Niu, K. Xue, Q. Zhao, and M.L. Ge, *The Role of the ℓ_1-Norm in Quantum Information Theory and Two Types of the Yang–Baxter Equation*, Journal of Physics A: Mathematical and Theoretical, **44**, 265304 (2011). G. Wang, K. Xue, C. Sun, C. Zhou, T. Hu, and Q. Wang, *Temperley–Lieb algebra, Yang–Baxterization and Universal Gate*, Quantum Information Processing, **9**, 699-710 (2010); C. Sun, G. Wang, T. Hu, C. Zhou, Q. Wang, and K. Xue, *The Representations of Temperley-Lieb Algebra and Entanglement in a Yang–Baxter System*, International Journal of Quantum Information, **7**, 1285-1293 (2009).

[36] M. V'elez and J. Ospina, *Generalized Temperley-Lieb Algebras and Quantum Computation*, Mathematical Theory and Computational Practice, 5th Conference on Computability in Europe, CiE 2009, Heidelberg, Germany, July 19-24, 2009.

[37] G. Wang, K. Xue, C. Sun, B. Liu, Y. Liu, and Y. Zhang, *Topological Basis Associated with B-M-W algebra: Two Spin-1/2 Realization*, Physics Letters A, **3**79, 1-4 (2015).